Master’ thesis

Development of Fitness-For-Service Assessment Method Based on Reliability

信頼性に基づく構造健全性評価手法の開発

37-116907 Qiang QU

Supervising Professor: Shinsuke SAKAI

Chapter 1. Introduction

1.1 Background

1.1.1 Fitness-For-Service and API standards

Fitness-For-Service (FFS) assessments are quantitative engineering evaluations that are performed to demonstrate the structural integrity of an in-service component containing a flaw or damage. The results of a FFS assessment can be used to make a run-repair-replace decision to ensure that the equipment with flaws that have been identified by inspection can continue to operate safely for some period of time [1].These FFS assessments are currently recognized and referenced by the API (American Petroleum Institute) Codes and Standards. API579 is a standard that was developed to evaluate flaws and damage associated with in-service operation. Besides, API510, API570, API 653, and NB-23 Codes/Standards are standards for the inspection, repair, alteration, and rerating of in-service equipment containing flaws.

API579 contains Fitness-For-Service (FFS) assessment procedures that can be used to evaluate pressurized components containing damage and flaws including metal loss, corrosion, and crack-like flaws.

1.1.2 Present status of FFS assessment of crack-like flaws

FFS assessment procedures using partial safety factors (PSFs) are provided in API579-1 [2] to determine the acceptability of crack-like flaws. These procedures are deterministic in that all information required for an analysis (independent variables as stress, toughness and crack dimension) are assumed to be known. Generally, the partial safety factors to be used are products of probabilistic analysis considering the specific condition of stress and structural geometries.

However, in many instances not all of the important independent variables are known with a high degree of accuracy (not enough data), otherwise there are difficulties to conduct probabilistic analysis (excessively complicated structural geometry). In such cases, a group of values of PSFs are given in API579 -1 to be used in the FFS assessment for an approximate evaluation. The API579 PSFs are shown in Table 3.2 in Chapter 3.

It is very convenient to use this existing group of API579 PSFs to evaluate various components with various structural geometries and crack geometries. However, these PSFs are calculated from the infinite plate model, if these PSFs are applied to evaluate real models of which the mechanical properties are different from an infinite plate, these differences in geometries may cause misestimating of the reliability or probability of failure (Pf) in the result of approximate evaluation. Thus these PSFs are permitted to be applied only when the underestimation of probability of failure is within an acceptable region.

However, the applicability (permit region) of these PSFs has not been clear. In order to promote the accuracy of the approximate evaluation, it is necessary and important to clarify the applicability of API579 PSFs, and develop applicable PSFs.

1.2 Objective and research direction

This paper investigates the applicability of AIP579-1 PSFs and develops new PSFs which could provide enough accuracy for an approximate evaluation of the safety margin.

For this purpose, we apply API579-1 PSFs to several concrete models to examine how the Pf changes from the target. Also PSFs of all these models including an infinite plate are calculated by the First Order Reliability Method (FORM), and compared to the API579-1 PSFs. A group of value of PSFs is generated from these calculated PSFs, and the applicability of this group of developed PSFs is also examined. Finally, sensitivity analysis is performed to investigate the dependence of the crack size on the Pf and the applicability of developed PSFs will be clarified.

Chapter 2. FFS Assessment of Crack-like Flaw

2.1 Assessment Procedures Using Partial Safety Factors

FFS assessment evaluating a crack-like flaw is based on the method using Partial Safety Factors and the Failure Assessment Diagram (FAD).

2.1.1 Partial Safety Factor (PSF)

In a deterministic deign, the safety factor is applied to the resistance in the safety check expression to ensure the capacity of system exceeds the loads. The expression is shown as follow.

$$\frac{R}{\gamma} \geq \sum_{i=1}^{n} L_i \tag{2.1}$$

where R is nominal resistance, L_i are various loads, and γ is the safety factor. Thus, this method doesn't provide a treatment of the uncertainties existing in strength and loads, and it is also unable to evaluate the actual safety margin by this method.

On the other hand, partial safety factors are individual safety factors that are applied to the independent variables in the safety expression.

$$\frac{R}{\varphi} \geq \sum_{i=1}^{n} \gamma_i \cdot L_i \tag{2.2}$$

where γ_i, φ are partial safety factors. These partial safety factors are developed using probabilistic analysis in which the resistance and loads are defined as random variables with distributions. The calculation of PSFs is based on reliability method considering a limit state model, distributions of the main independent variables of the model, and a target reliability or probability of failure (see paragraph 2.2). Hence, the uncertainties of loads and resistance can be treated by separately combining the nominal value of each variable with its own partial safety factor, and also the safety margin is introduced by the target reliability or probability of failure [3].

2.1.2 Failure Assessment Diagram

Failure Assessment Diagram is a convenient, technically based method which is used for the evaluation of crack-like flaws in components. The FAD approach provides a measure for the acceptability of a component with a crack-like flaw when the failure mechanism is measured by two distinct criteria: unstable fracture and limit load. Unstable fracture usually controls failure for small flaws in components fabricated from a brittle material and plastic collapse typically controls failure for large flaws if the component is fabricated from a material with high toughness [2].

In a FAD analysis of crack-like flaws, the results from a stress analysis, stress the material strength, and fracture toughness are combined to calculate a toughness ratio, *Kr* , and load ratio, *Lr*.

$$K_r = \frac{Y(a)\sqrt{\pi a}\left(\frac{S^P}{\sigma_y} + \frac{\Phi_P S^S}{\sigma_y}\right)}{\frac{K_{mat}}{\sigma_y}} \tag{2.3}$$

$$L_r = \frac{L(a)S^P}{\sigma_y} \tag{2.4}$$

where *Y(a)* and *L(a)* are geometry indices; *a* is the crack dimension; S^P is primary stress and S^S is second stress; K_{mat} is toughness value; Φ_P is the plasticity interaction factor, σ_y is yield stress.

These two quantities represent the coordinates of a point that is plotted on a two dimensional FAD to determine acceptability of a crack-like flaw. As shown in Figure 2.1, if the assessment point is on or below the FAD curve, the crack-like flaw won’t cause a failure during the operation.

2.1.3 FFS assessment procedures using PSF

In the FFS assessment of crack-like flaws, the acceptance of flaw is determined by the satisfaction of reliability. In assessment procedures, partial safety factors are used along with the FAD to examine whether the target reliability is reached.

Three separate partial safety factors are used: a factor for applied loading PSF_S (γ_S);

a factor for material toughness PSF_K (γ_K); and a factor for flaw dimension PSF_a (γ_a). These partial safety factors are applied to the stresses, the fracture toughness and the flaw size parameters prior to conducting a FAD analysis.

$$S^S = S^S \cdot \gamma_S \tag{2.5}$$

$$S^S = S^S \cdot \gamma_S \tag{2.6}$$

$$K_{mat} = K_{mat} / \gamma_K \tag{2.7}$$

$$a = a \cdot \gamma_a \tag{2.8}$$

K_r and L_r are computed by equation 2.1 and 2.2, and plotted on the FAD to conduct the FAD assessment. If the assessment point is on or below the FAD curve, the target reliability responding with the partial safety factors is satisfied, the crack-like flaw is acceptable, and the component is suitable for continued operation. A schematic that illustrates the procedure for FFS assessment of a crack-like flaw using the Failure Assessment Diagram and PSFs is shown in Figure 2.2

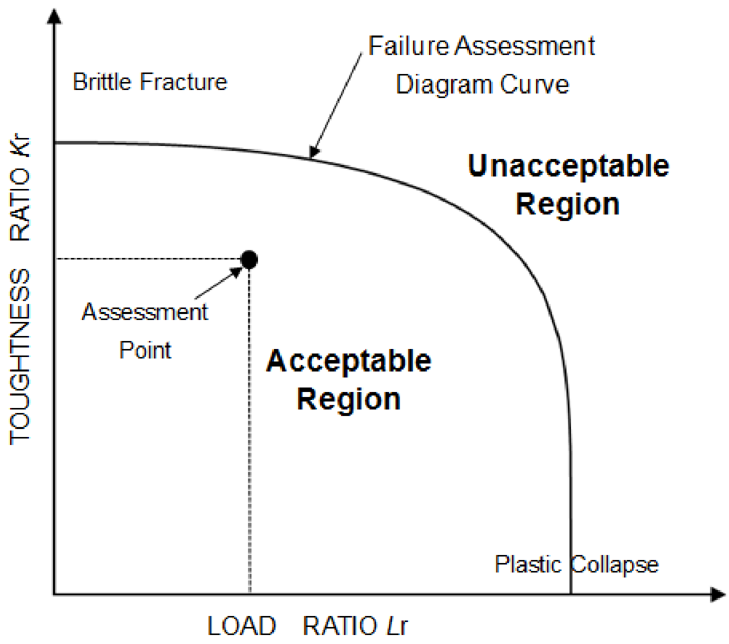

Figure 2.1 Failure assessment diagram analysis

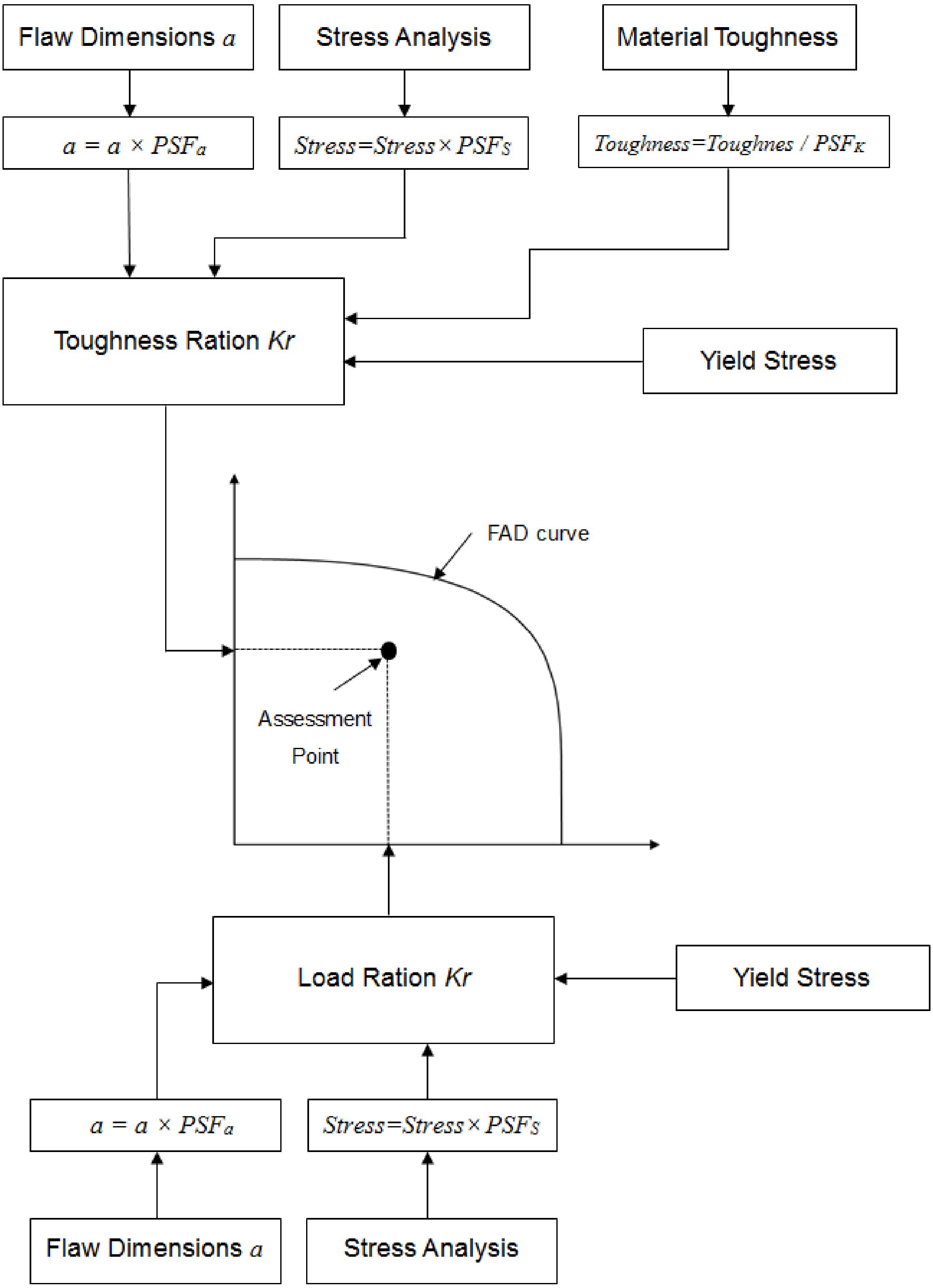

Figure 2.2 FFS assessment procedures

2.2 Probabilistic approaches of PSF derivation

A probabilistic approach to evaluate the reliability of component is introduced, and the calculation of PSFs based on this approach is also introduced in this paragraph.

2.2.1 Limit state function

The limit state is defined as the boundary between the safe and unsafe region in the design parameter space. In FFS assessment, as previously described in 2.1, the acceptability of a crack-like flaw is determined by that assessment point is inside or outside the FAD curve. Hence the FAD curve defines the limit state, and the distance from assessment point to this curve is used to define the limit state function.

The limit state function is defined as follow.

$$g = r - \sqrt{K_r^2 + L_r^2} \tag{2.9}$$

where r is the distance from O to FAD curve, and $\sqrt{K_r^2 + L_r^2}$ is distance o assessment point.

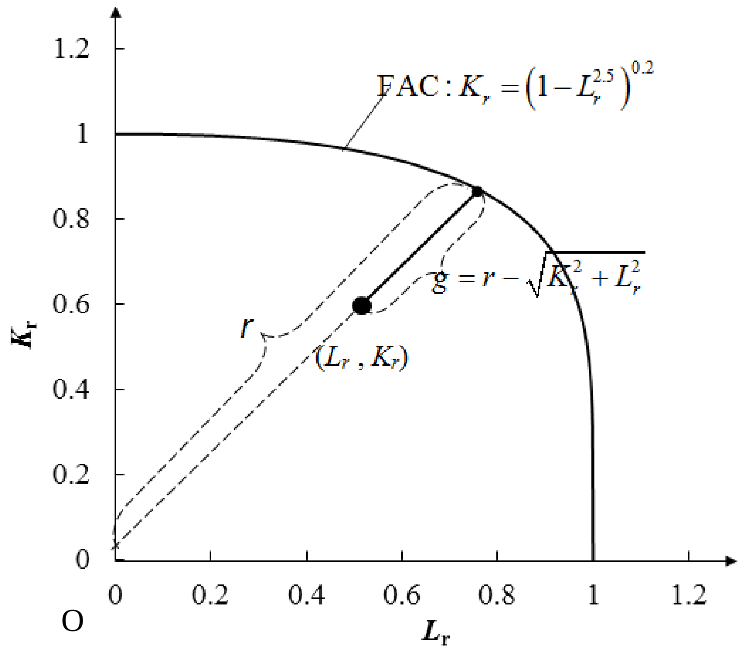

Figure 2.3 Definition of limit state function

2.2.2 Reformulation of limit state function

In order to facilitate the use of reliability computer program to solve for the PSFs, the limit state function is re-derived in terms of normalized random variables of stress, toughness and crack dimension.

The primary stress is defined as a distribution having a mean value of $\mu_{S,}$ and standard deviation of σ_S (in this reformulation, the secondary stress is not a random variable).

$$S^P \Rightarrow DIS\left[\mu_S, \sigma_S\right] \tag{2.10}$$

A new random variable can be described using the following equations.

$$X = \frac{S^P}{\mu_S} \tag{2.11}$$

$$X \Rightarrow DIS\left[1.0, COV_S\right] \tag{2.12}$$

where the *COV* (Coefficient Of Variation) is defined by $COV = \mu/\sigma$. It represents the ratio of the standard deviation to the mean, and it is a useful statistic for comparing the degree of variation and an important index to show the uncertainties of variables.

A similar transformation can be made for the fracture toughness.

$$K_{mat} \Rightarrow DIS\left[\mu_K, \sigma_K\right],\ \ Y = \frac{K_{mat}}{\mu_K},\quad Y \Rightarrow DIS\left[1.0, COV_K\right] \tag{2.13}$$

Define the constants A and R_{ky} as follows

$$A = \frac{\mu_S}{\sigma_y},\quad R_{ky} = \frac{\mu_K}{\sigma_y} \tag{2.14}$$

Using the equation 2.1, 2.2, 2.11, 2.14, the limit state function finally reworked as follow

$$g = r - L(a) AX \sqrt{1 + \left(\frac{Y(a)\sqrt{\pi a}}{L(a) R_{ky} Y} \right)^2} \quad (2.15)$$

where, $L(a)$ and $Y(a)$ are functions of crack dimension. Though stress analyses, $L(a)$ and $Y(a)$ are obtained. For different models, the $L(a)$ and $Y(a)$ are different. As a result, the limit state functions are different for all the models.

2.2.3 Calculation of partial safety factors

In a probabilistic approach, the basic design criterion is either a maximum allowable probability of failure (target Pf) or a minimum allowable reliability index β (target reliability β_0). Two factors are related as the equation given follow

$$Pf = \Phi(-\beta_0) \quad (2.16)$$

where Φ is the standard normal cumulative distribution function (CDF).

A general calculating method of partial safety factors is reliability method including first order reliability method (FORM) and second order reliability method (SORM). In reliability method, for nonlinear limit state, the computation of the minimum value of reliability index becomes an optimization problem:

$$\begin{aligned} &\text{Minimize } \beta = \sqrt{u^T u} \\ &\text{Subject to } g(u) \le 0 \end{aligned} \quad (2.17)$$

where ***u*** is a vector of standardized variables.

The algorithm process is required to change the parameter *A*, *B* manually until the target reliability is satisfied ($\beta = \beta_0$). The outputs of this calculation includes the direction cosines ($\alpha_X^*, \alpha_Y^*, \alpha_a^*$), and design point values (X^*, Y^*, a^*) which are used to derive the PSFs using the following equations.

$$\gamma_X = \frac{X^*}{\mu_x}, \quad \gamma_K = \frac{\mu_Y}{Y^*}, \quad \gamma_a = \frac{a^*}{\mu_a} \quad (2.18)$$

Then, using the equation 2.11 and 2.13 to calculate the PSFs of stress and toughness, the PSFs are obtained as

$$\gamma_S = \frac{\gamma_X \cdot \mu_S}{\mu_S} = \gamma_X\ , \quad \gamma_K = \frac{\mu_K}{\mu_K / \gamma_Y} = \gamma_Y \tag{2.19}$$

These tree partial safety factors are applied to the FFS assessment according to the procedures introduced in 2.13. In Chapter 4, this reliability approaches are used to calculate PSFs of several models.

Chapter 3. Applicability Investigation of API579 PSFs

3.1 Applicability investigation process

3.1.1 API579 PSFs

As introduced in the paragraph 1.1.2, in API579-1, a group of values of PSFs are given to be used for an approximate evaluation in the FFS assessment. These PSFs are shown in Table 3.2. In this table, for the shallow cracks, 18 cases of PSFs divided by combining 3 target reliability levels, 3 categories of uncertainty in primary stress (COV_S), 2 failure regions (R_{ky}>R_c, plastic collapse region; R_{ky}< R_c, brittle fracture region) are given, as well as another 18 cases for the deep cracks are also given.

These PSFs are calculated from an infinite plate model of which the geometry indices $L(a)$ and $Y(a)$ are constant 1.0. Apply these PSFs to real models of which $L(a)$ and $Y(a)$ are functions of crack dimension, the dependence of crack dimension on the Pf is weakened and the design point changes in a reliability approaches, finally an underestimation of Pf is resulted. If the underestimation of Pf is acceptable, it is still reasonable for us to apply API579 PSFs in the evaluation.

In the derivation of API579 PSFs, random distributions of the independent variables of stress, toughness and crack dimension are assumed as shown in Table 3.1.

Table 3.1 Independent variables of the derivation of API579 PSFs [4]

Variable	Distribution	Mena value	COV
Crack size (mm)	Lognormal	2.5	0.3
Fracture toughness	Weibull	1	0.25
Primary membrane stress	Gunbel	1	0.1,0.2,0.3

Table 3.2 Partial Safety Factors given in API579-1

Shallow Cracks *a*<5mm (0.2 *inches*)								
β	**COVs**	**R_c***	**$R_{ky}<R_c$**			**$R_{ky}>R_c$**		
			PSFs	**PSFk**	**PSFa**	**PSFs**	**PSFk**	**PSFa**
2	**0.1**	**0.5**	**1.20**	**1.43**	**1.08**	**1.25**	**1.0**	**1.0**
	0.2	**0.5**	**1.30**	**1.43**	**1.08**	**1.50**	**1.0**	**1.0**
	0.3	**0.5**	**1.55**	**1.43**	**1.08**	**1.75**	**1.0**	**1.0**
3.09	**0.1**	**0.7**	**1.40**	**1.43**	**1.20**	**1.50**	**1.0**	**1.0**
	0.2	**0.7**	**1.50**	**1.82**	**1.10**	**2.00**	**1.0**	**1.0**
	0.3	**0.7**	**2.00**	**2.00**	**1.05**	**2.50**	**1.0**	**1.0**
4.75	**0.1**	**1.1**	**1.75**	**2.00**	**1.35**	**2.00**	**1.0**	**1.0**
	0.2	**1.1**	**2.50**	**2.00**	**1.50**	**3.10**	**1.0**	**1.0**
	0.3	**1.1**	**2.60**	**2.00**	**1.50**	**4.10**	**1.0**	**1.0**
Deep Cracks *a*>5mm (0.2 *inches*)								
β	**COVs**	**Rc**	**$R_{ky}<R_c$**			**$R_{ky}>R_c$**		
			PSFs	**PSFk**	**PSFa**	**PSFs**	**PSFk**	**PSFa**
2	**0.1**	**0.5**	**1.20**	**1.33**	**1.10**	**1.25**	**1.0**	**1.0**
	0.2	**0.5**	**1.40**	**1.54**	**1.10**	**1.50**	**1.0**	**1.0**
	0.3	**0.5**	**1.60**	**1.67**	**1.10**	**1.75**	**1.0**	**1.0**
3.09	**0.1**	**0.7**	**1.40**	**1.67**	**1.15**	**1.50**	**1.0**	**1.0**
	0.2	**0.7**	**1.80**	**1.43**	**1.10**	**2.00**	**1.0**	**1.0**
	0.3	**0.7**	**2.30**	**1.43**	**1.10**	**2.50**	**1.0**	**1.0**
4.75	**0.1**	**1.1**	**1.70**	**2.00**	**1.25**	**2.00**	**1.0**	**1.0**
	0.2	**1.1**	**2.60**	**1.82**	**1.25**	**3.10**	**1.0**	**1.0**
	0.3	**1.1**	**3.50**	**1.67**	**1.25**	**4.10**	**1.0**	**1.0**

Notes:

✶ R_c is a cut-off value used to define the regions of brittle fracture and plastic collapse. The values of R_c has been conversed to IU (international unit).

3.1.2 Investigation process

In order to make clear the applicability, API579 PSFs are applied to 7 real models to investigate whether the reliability or probability of failure is evaluated precisely. The investigation is performed according to the following steps

[1]. A limit state function of real model is defined (the geometry indices $L(a)$ and $Y(a)$ are used the theoretical expressions given in API579 Appendix).

$$g\left(X, Y, a, A, R_{ky}\right) = 0 \tag{3.1}$$

[2]. Determine the target reliability β_0 and COV_S, and choose PSFs from Table 3.1. Apply the PSFs to the variables, and conduct a FAD analysis. Find the maximum of allowable K_r for each L_r. Otherwise, we can find the (A_{max}, R_{ky}) instead of point of (Lr, K_{rmax}).

$$g\left(X \cdot \gamma_X, Y \cdot \gamma_Y, a \cdot \gamma_a, A, R_{ky}\right) = 0 \tag{3.2}$$

[3]. Evaluate reliability or Pf of the assessment point (Lr, K_{rmax}) by first order reliability method (FORM).

When we apply API579 PSFs in the evaluation, every assessment point inside or on the $g\left(X_i \cdot \gamma_i\right) = 0$ curve are considered to be acceptable because the target reliability is satisfied. However, if we perform a FORM to draw a reliability contour line of β_0, the result shows that some of the assessment points are on the contour line; while some are out of the reliability contour line as shown in Figure 3.1. The reliability of these outside points are not actually reaching the target reliability β_0, and in these cases, using the API579 PSFs will cause a wrong accepting decision of the crack-like flaws. So in these cases, API579 should not be applied in the evaluation.

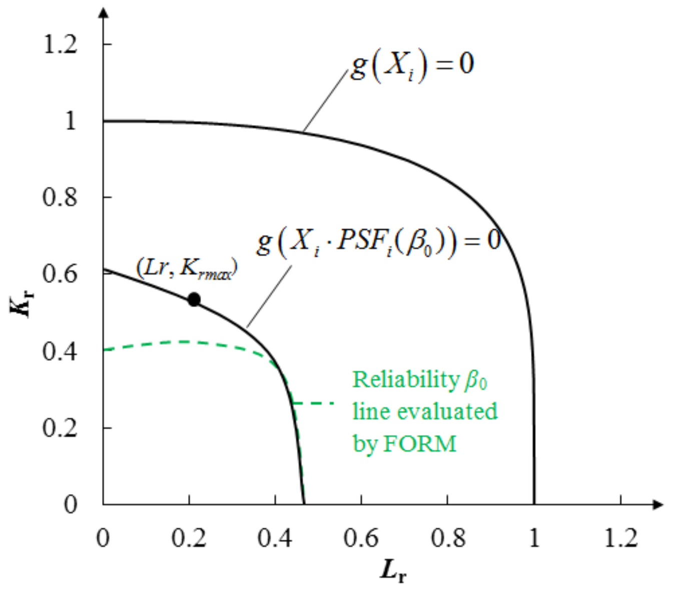

Figure 3.1 Misestimating of reliability caused by API579 PSFs

3.2 Results

We investigated the applicability of API579 PSFs for 7 models including plates and cylinders containing surface cracks. We use a crack depth- to-wall thickness ratio (*a*/*t*) instead of nominal depth to show the crack changes from shallow to deep. If the *a*/*t* is deeper than 0.3, we consider it as a deep crack and choose the PSFs from its category in Table 3.2. Results of applicability investigation of 3 real models are given in this paragraph.

3.2.1 Model 1: Plate containing semi-elliptical shape surface crack subjected to membrane stress

Model 1 is a plate containing a semi-elliptical shape surface crack which is shown in Figure 3.2.

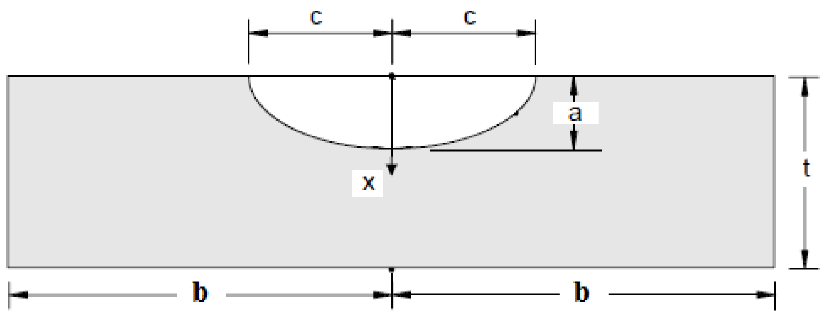

Figure 3.2 Plate containing semi-elliptical shape surface crack [2]

The geometry indices of $Y(a)$ and $L(a)$ are defined according to the existing expression given in API579 as follows

$$Y(a)=\frac{\left[1.13-0.09\frac{a}{c}+\left\{-0.54+\frac{0.89}{0.2+a/c}\right\}\left(\frac{a}{t}\right)^{2}+\left\{0.5-\frac{1}{0.65+a/c}+14\left(1-\frac{a}{c}\right)^{24}\right\}\left(\frac{a}{t}\right)^{4}\right]\left[\sec\left(\frac{\pi c}{2b}\sqrt{\frac{a}{t}}\right)\right]^{\frac{1}{2}}}{\sqrt{1+1.464\left(\frac{a}{c}\right)^{1.65}}} \quad (3.1)$$

$$L(a)=\left(1-\frac{ac}{t(c+t)}\right)^{-0.42} \quad (3.2)$$

The plate length b and crack length c are assumed as $b=3c=6a$ in this investigation. We investigate the cases when a/t = 0.1, 0.2, 0.3 for each categories of API579 PSFs. We show the misestimating in the evaluation by using the probability of failure which provides a more intuitionistic observation.

In Figure 3.3 (a, b, c), the cases of target β=2.0 (Pf=2.3×10^{-2}), COV_S=0.1, 0.2, 0.3 have been shown. It can be seen that, in the brittle fracture region, the Pf are greater than the target Pf, and with the increase of crack depth, this Pf is getting farther from the target Pf. It is also shown that, when the COV_S is chosen a high level, the underestimation in Pf becomes less. In contrast, in the plastic collapse region, the Pf are nearly agreeing with the target Pf.

Results of higher target reliability levels are shown in Figure 3.4 and Figure 3.5. The same characteristics are obtained as the cases β=2.0. However, for a higher reliability level, the underestimation of Pf is becoming relatively huge.

It can be concluded that, when we evaluate a plate component containing semi-elliptical surface crack, if the material is a low toughness material for which the failure model is more likely a brittle fracture, the API579 PSFs should not be applied in the evaluation because the actual probability of failure is greater than that expected; while if the material is a high toughness material (plastic collapse region), the API579 PSFs are applicable.

(a)

(b)

(c)

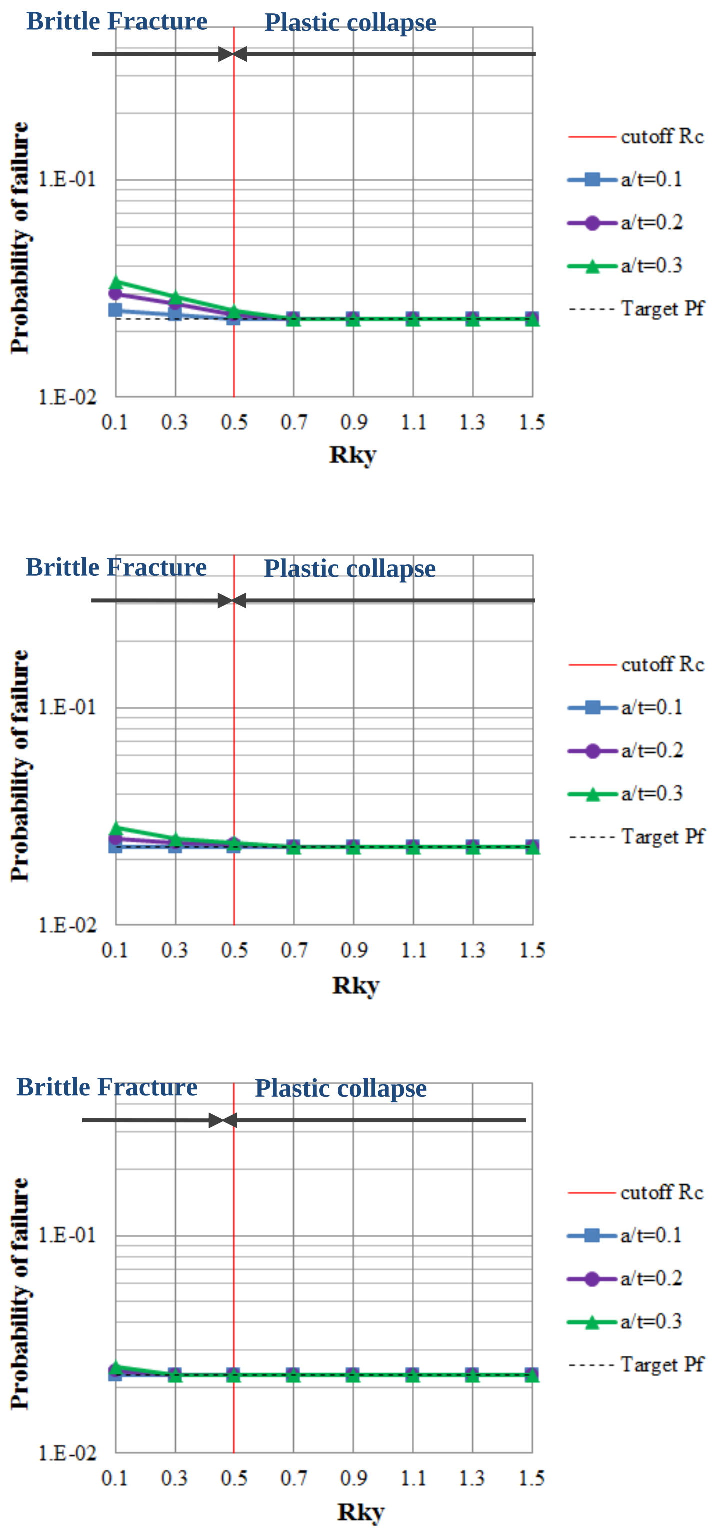

Figure 3.3 Underestimation of Pf when API579 PSFs are applied to model 1 for the cases that target β=2.0 (Pf=0.023), (a) *COVS*=0.1, (b) *COVS*=0.2, (c) *COVS*=0.3

(a) (b) (c)

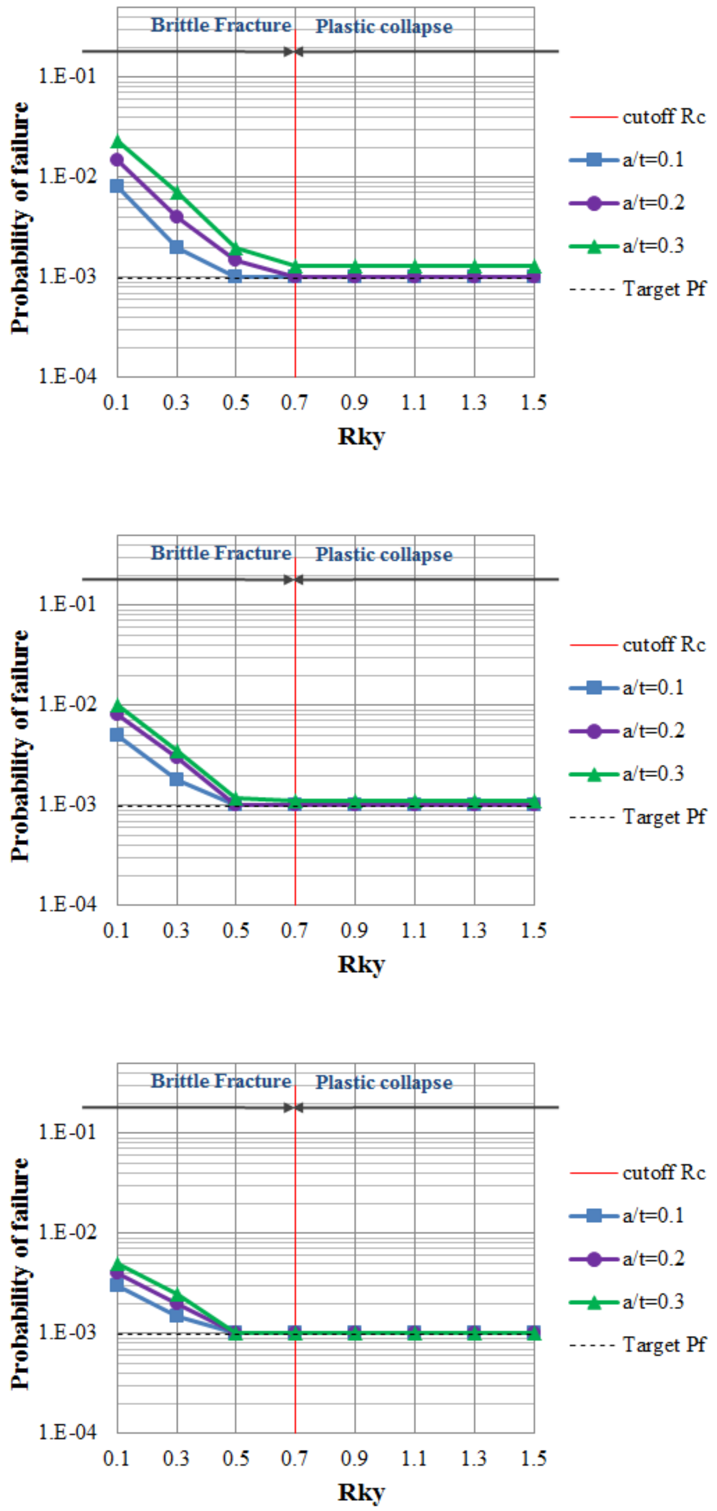

Figure 3.4 Underestimation of Pf when API579 PSFs are applied to model 1 for the cases that target β=3.09 (Pf=0.001), (a) *COVS*=0.1, (b) *COVS*=0.2, (c) *COVS*=0.3

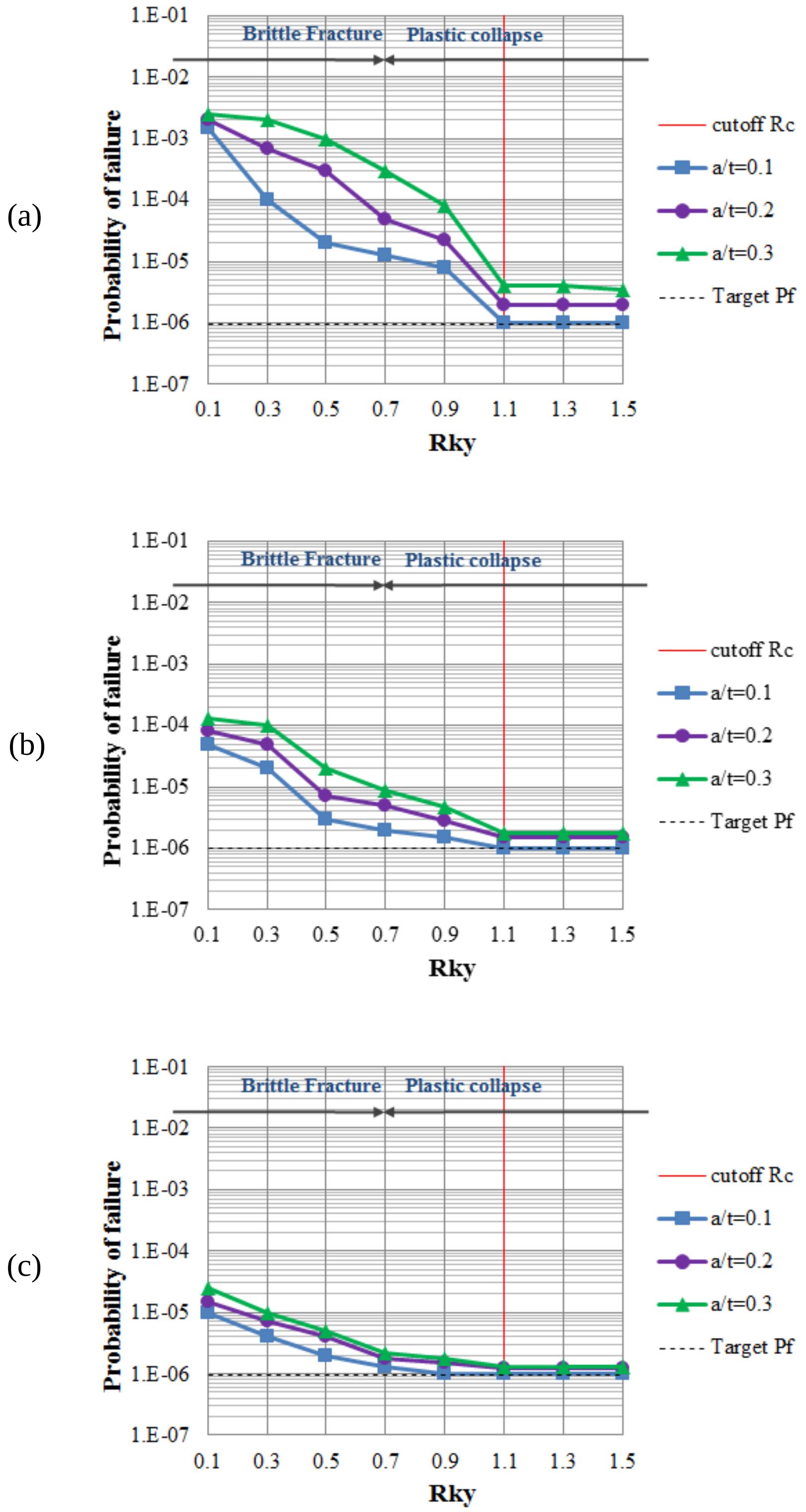

Figure 3.5 Underestimation of Pf when API579 PSFs are applied to model 1 for the cases that target β=4.75 (Pf=10^{-6}), (a) *COVS*=0.1, (b) *COVS*=0.2, (c) *COVS*=0.3

3.2.2 Model 2: Plate containing infinite long surface crack subjected to membrane stress

Model 2 is a plate containing infinite length surface crack which is shown in Figure 3.6.

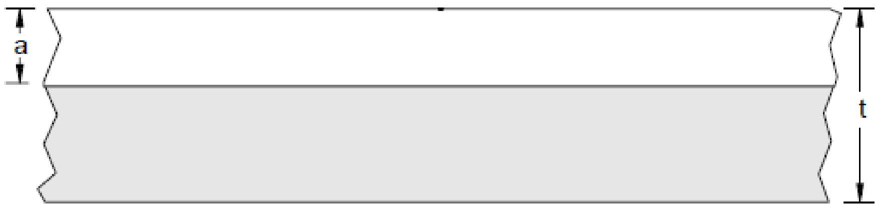

Figure 3.6 Plate containing infinite long shape surface crack [2]

The geometry indices of $Y(a)$ and $L(a)$ are also defined according to the existing expression given in API579 as follows

$$Y(a)=\frac{\left\{0.752+2.02\frac{a}{t}+0.37\left[1-\sin\left(\frac{\pi a}{2t}\right)\right]\right\}\left[\frac{2t}{\pi a}\tan\left(\frac{\pi a}{2t}\right)\right]^{\frac{1}{2}}}{\cos\left(\frac{\pi a}{2t}\right)} \tag{3.3}$$

$$L(a)=\frac{\frac{a}{t}+\sqrt{1-2\frac{a}{t}+2\left(\frac{a}{t}\right)^2}}{\left(1-\frac{a}{t}\right)^2} \tag{3.4}$$

The results of 9 cases of combination of target β (2.0, 3.09, 4.75) and COV_S (0.1, 0.2, 0.3) are shown in Figure 3.7, 3.8, and 3.9.

Comparing with the model 1, the Pf increases obviously even when the crack is a shallow crack.

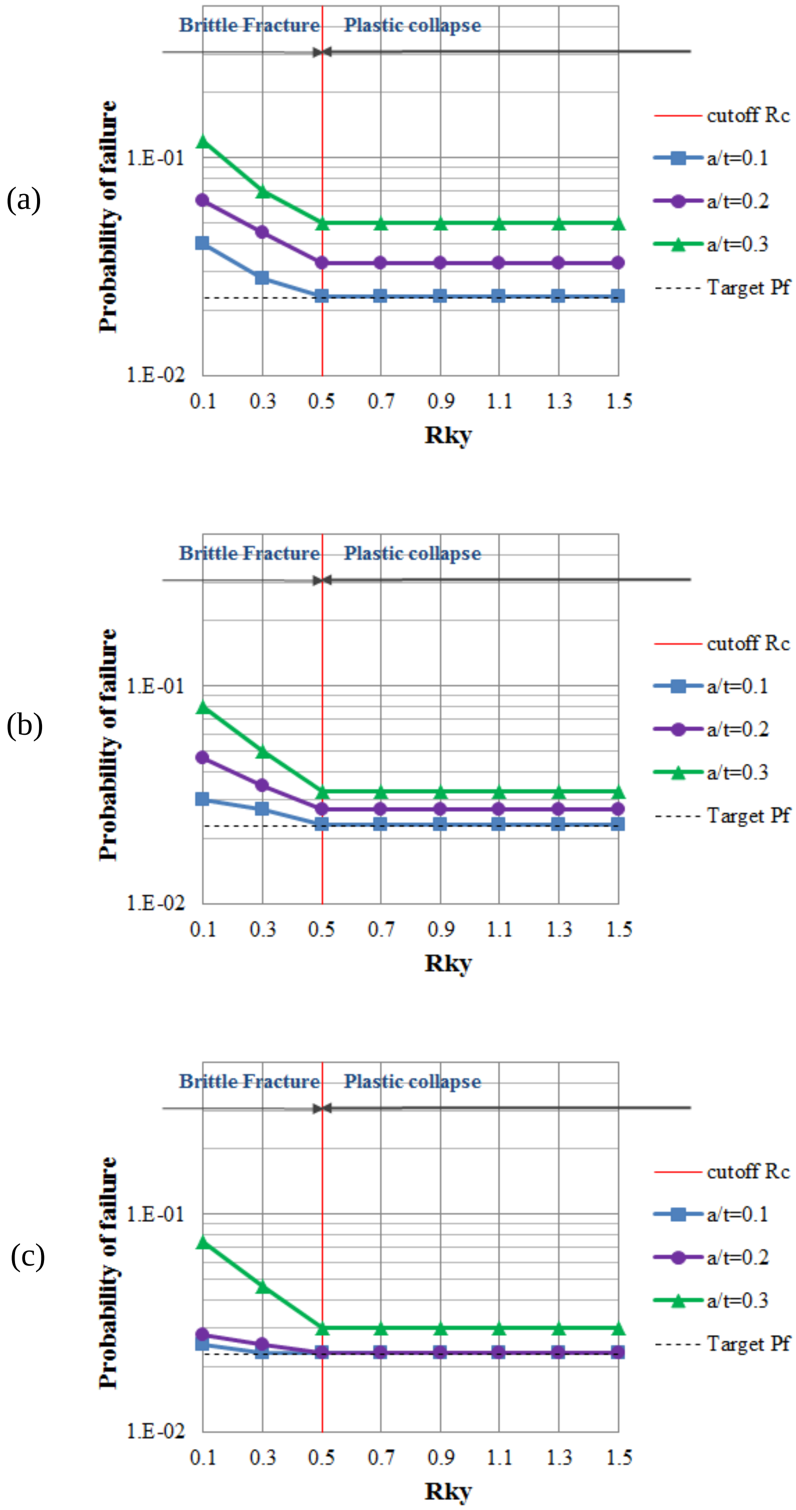

Figure 3.7 Underestimation of Pf when API579 PSFs are applied to model 2 for the cases that target β=2.00 (Pf=0.023), (a) *COVS*=0.1, (b) *COVS*=0.2, (c) *COVS*=0.3

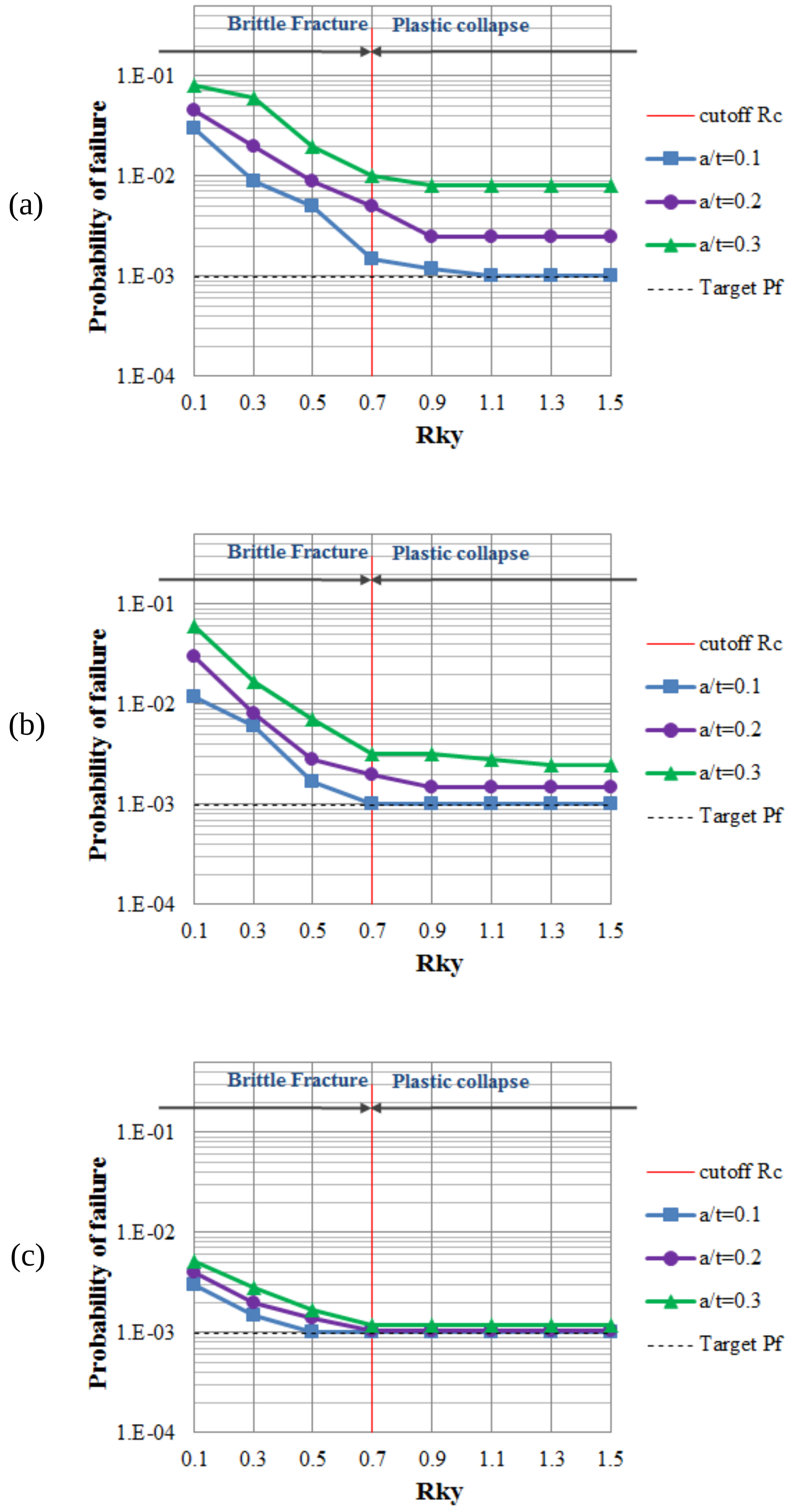

Figure 3.8 Underestimation of Pf when API579 PSFs are applied to model 2 for the cases that target β=3.09 (Pf=0.001), (a) *COVS*=0.1, (b) *COVS*=0.2, (c) *COVS*=0.3

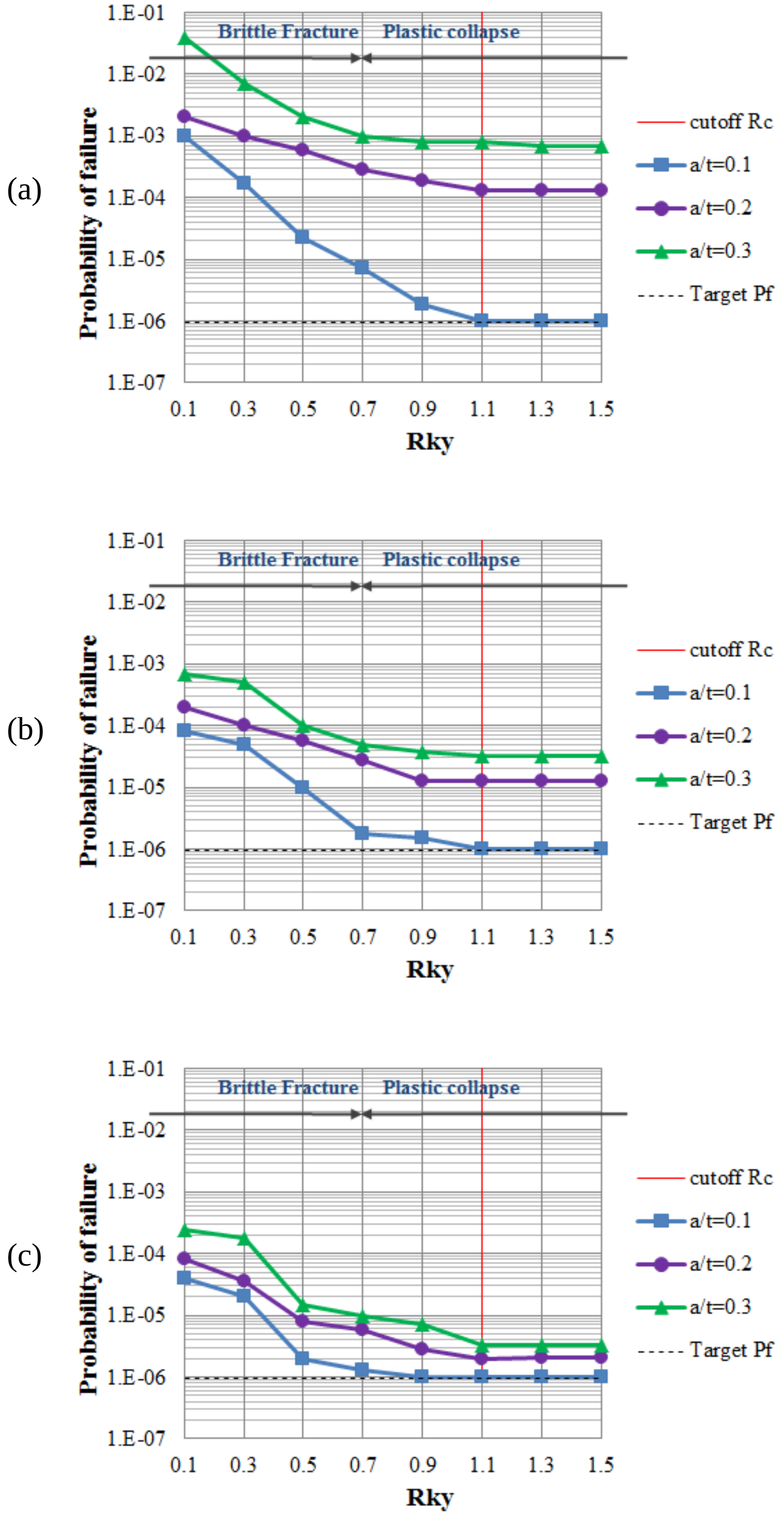

Figure 3.9 Underestimation of Pf when API579 PSFs are applied to model 2 for the cases that target β=4.75 (Pf=10^{-6}), (a) *COVS*=0.1, (b) *COVS*=0.2, (c) *COVS*=0.3

3.2.3 Model 3: Cylinder containing longitudinal direction, infinite length surface crack subjected to inner pressure

Model 2 is a Cylinder containing longitudinal direction, infinite length surface crack as shown in Figure 3.10.

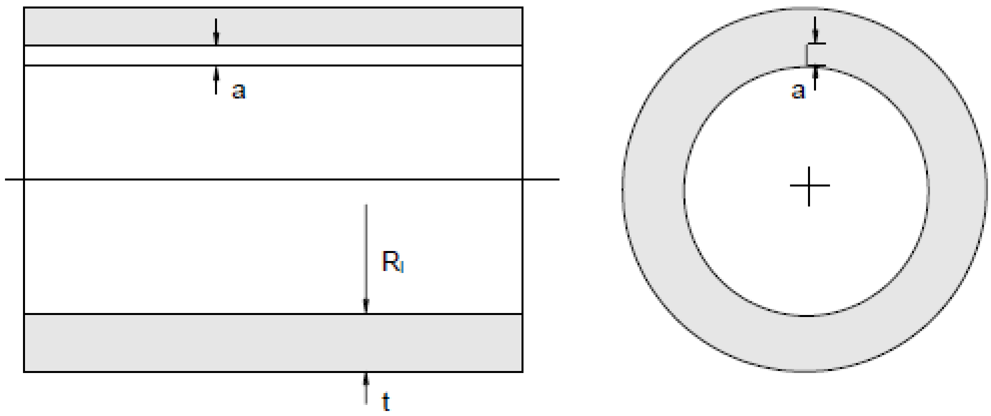

Figure 3.10 Cylinder – Surface Crack, Longitudinal Direction, Infinite Length [2]

The geometry indices of $Y(a)$ and $L(a)$ are also defined according to the existing expression given in API579 as follows

$$Y(a) = 1.1 + \alpha\left[4.95\left(\frac{a}{t}\right)^2 + 1.092\left(\frac{a}{t}\right)^4\right]$$

$$\alpha = \begin{cases} \left(0.2\dfrac{R_i}{t} - 1\right)^{0.25} & 10 \le \dfrac{R_i}{t} \le 20 \\ \left(0.125\dfrac{R_i}{t} - 0.25\right)^{0.25} & 5 \le \dfrac{R_i}{t} < 10 \end{cases} \tag{3.5}$$

$$L(a) = \frac{\dfrac{a}{t} + \sqrt{1 - 2\dfrac{a}{t} + 2\left(\dfrac{a}{t}\right)^2}}{\left(1 - \dfrac{a}{t}\right)^2} \tag{3.6}$$

The Ri/t is assumed to be 10 in this investigation. The results of 9 cases of combination of target β (2.0, 3.09, 4.75) and COV_S (0.1, 0.2, 0.3) are shown in Figure 3.11, 3.12, and 3.13.

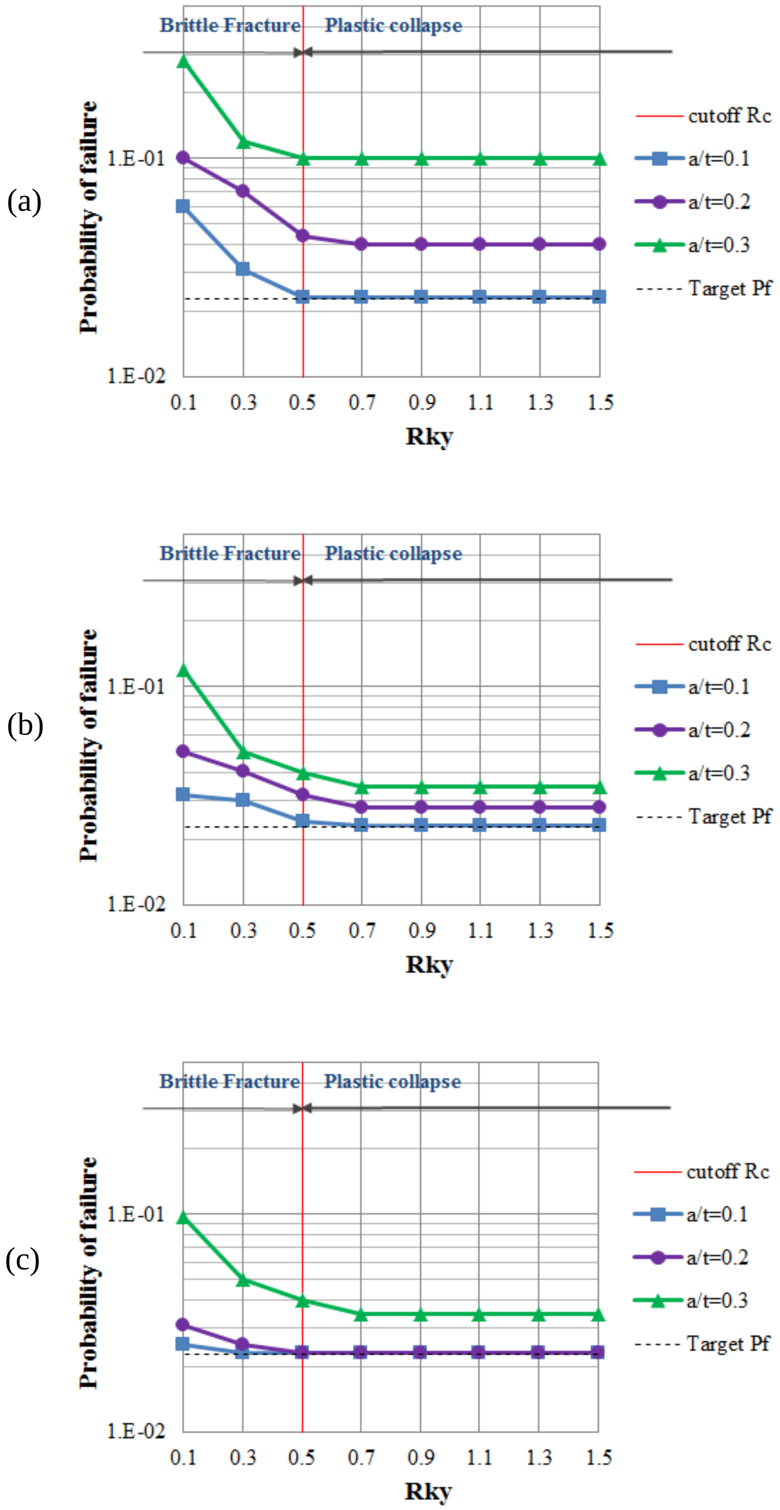

Figure 3.11 Underestimation of Pf when API579 PSFs are applied to model 3 for the cases that target β=2.0 (Pf=0.023), (a) *COVS*=0.1, (b) *COVS*=0.2, (c) *COVS*=0.3

(a)

(b)

(c)

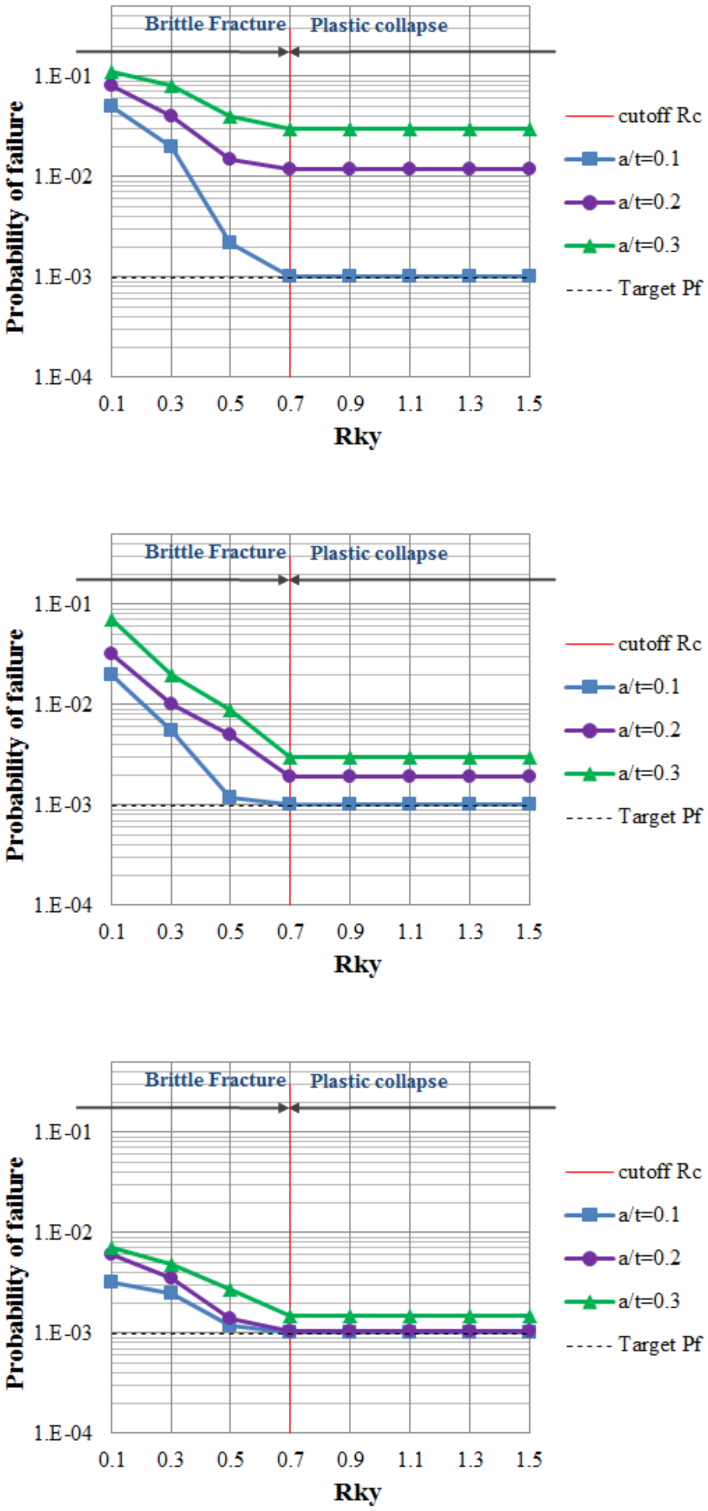

Figure 3.12 Underestimation of Pf when API579 PSFs are applied to model 3 for the cases that target β=3.09 (Pf=0.001), (a) *COVS*=0.1, (b) *COVS*=0.2, (c) *COVS*=0.3

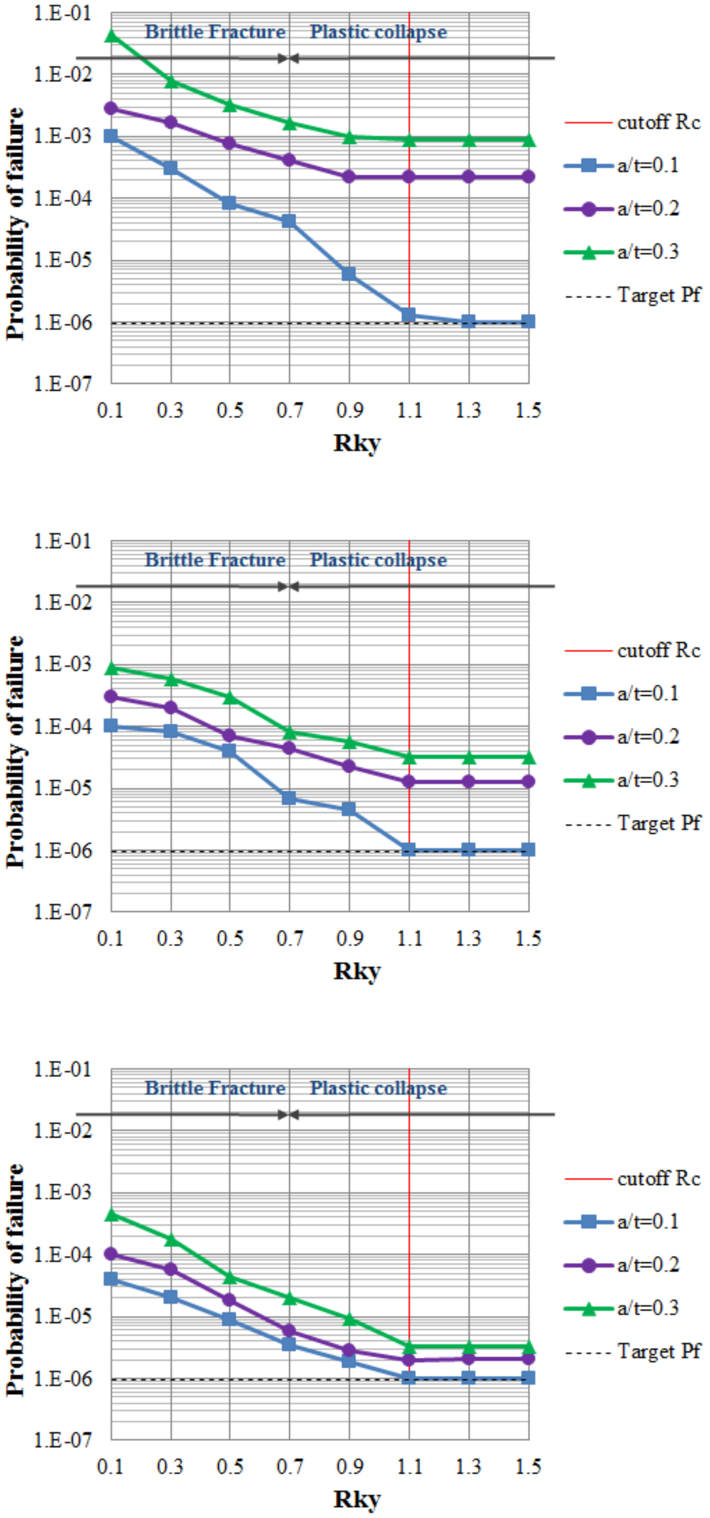

Figure 3.13 Underestimation of Pf when API579 PSFs are applied to model 3 for the cases that target β=4.75 (Pf=10^{-6}), (a) *COVS*=0.1, (b) *COVS*=0.2, (c) *COVS*=0.3

3.2.4 Other models

We also investigate the applicability of API579 PSFs for other 4 models including 1) cylinder containing inner longitudinal direction semi-elliptical surface crack 2) cylinder containing inner circumferential direction semi-elliptical surface crack, 3) inner circumferential direction long surface crack, 4) embedded circumferential direction long surface crack.

The results are nearly same as those of 3 models given above. In the region of brittle fracture, the Pfs are not evaluated precisely by the API579, therefore these PSFs should not be applied to evaluate the real models; while in the region of plastic collapse region, when the crack is shallow (elliptical surface crack: a/t <0.3; long surface crack: a/t <0.1), these API579 PSFs are applicable.

Chapter 4. Development of Partial Safety Factors

4.1 PSF calculations of models

4.1.1 PSFs calculated from real models

Results given in Chapter 3 showed that the API579 PSFs are not able to evaluate the Pf precisely in most of the cases. It is necessary to develop a new group of PSFs to be used for an approximate evaluation. For this purpose, we calculate actual PSFs for the real models, and generate a new group of new PSFs from these PSFs. The methodology has been introduced in Chapter 2, and the random independent variables are assumed as the same as shown in Table 3.1.

The calculation results of model 1, when the target reliability $\beta_0 = 3.09$, $COV_S = 0.1$, $a/t = 0.1, 0.2, 0.3$ are shown in Figure 4.1. It can be seen that when the crack depth increases, the PSFs of crack dimension reach a higher value; while the PSFs of stress and toughness change oppositely.

The results of model 2 when the target reliability $\beta_0 = 3.09$, $COV_S = 0.1$, $a/t = 0.1$, 0.2, 0.3 are shown in Figure 4.2. The PSFs are changes enormously when the crack gets deeper. The results of model 3 of the same case are shown in Figure 4.3.

It is shown in 3 groups of results that when the crack depth increases, in the region of brittle fracture, the PSF of crack dimension increased, and the PSF of toughness decreased; while in the region of plastic collapse, the PSF of crack dimension also increased, and the PSF of stress decreased. This is because the increase in crack depth enhanced the dependence of crack dimension on the probability of failure, and the dependences of other variables were relatively weakened.

It also can be seen that in the brittle fracture region, the PSFs are calculated by FORM is not as the same as the PSFs given in API579; while in the plastic collapse region, the PSFs of shallow cracks are nearly agreeing with the API579 PSFs. Reviewing the results shown in Chapter 3, this disagreements of PSFs resulted the misestimating of Pf.

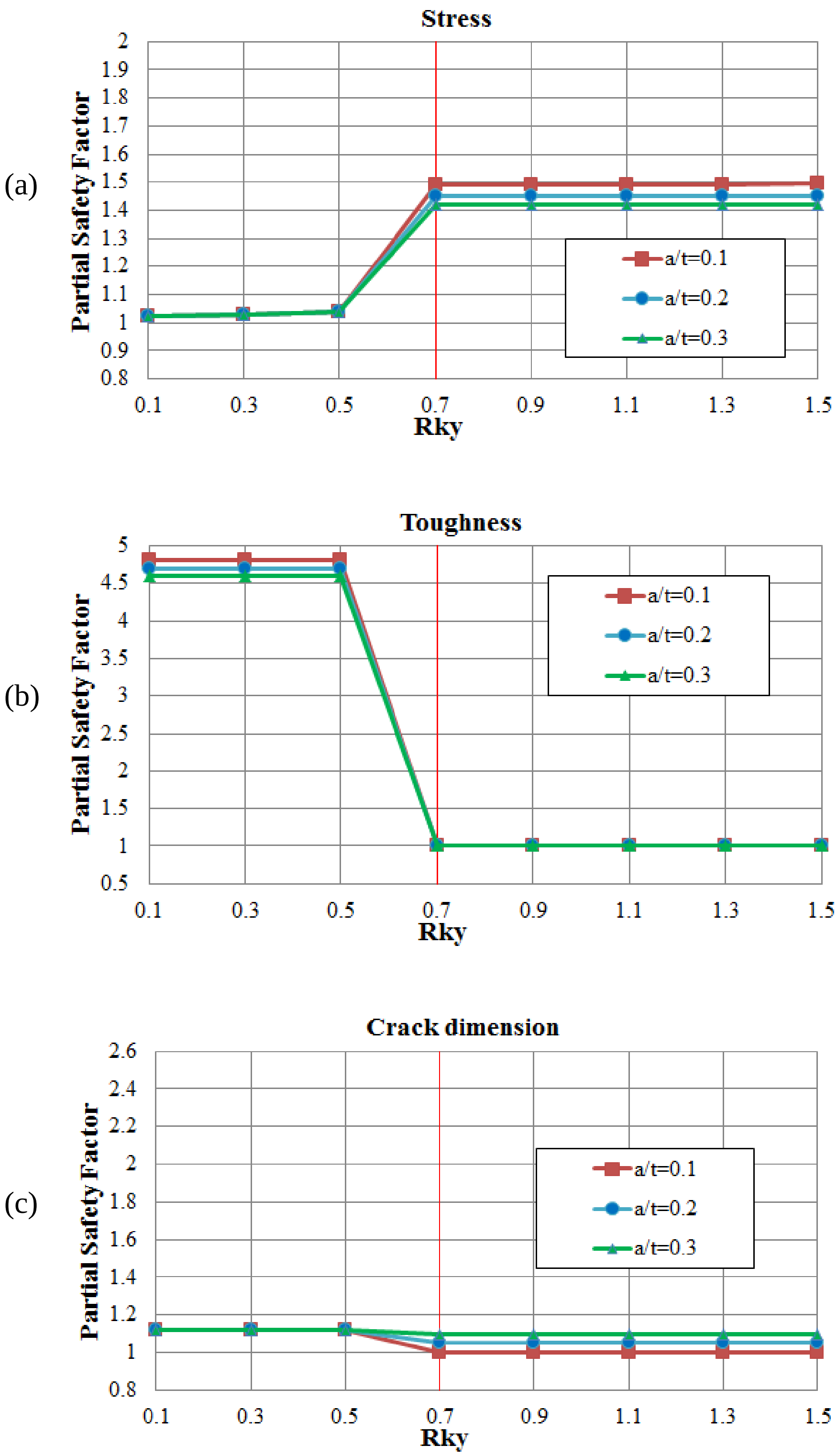

Figure 4.1 PSFs of model 1 whenβ_0 = 3.09, COV_S = 0.1, a/t = 0.1, 0.2, 0.3, (a) PSF of stress, (b) PSF of toughness, (c) PSF of crack dimension

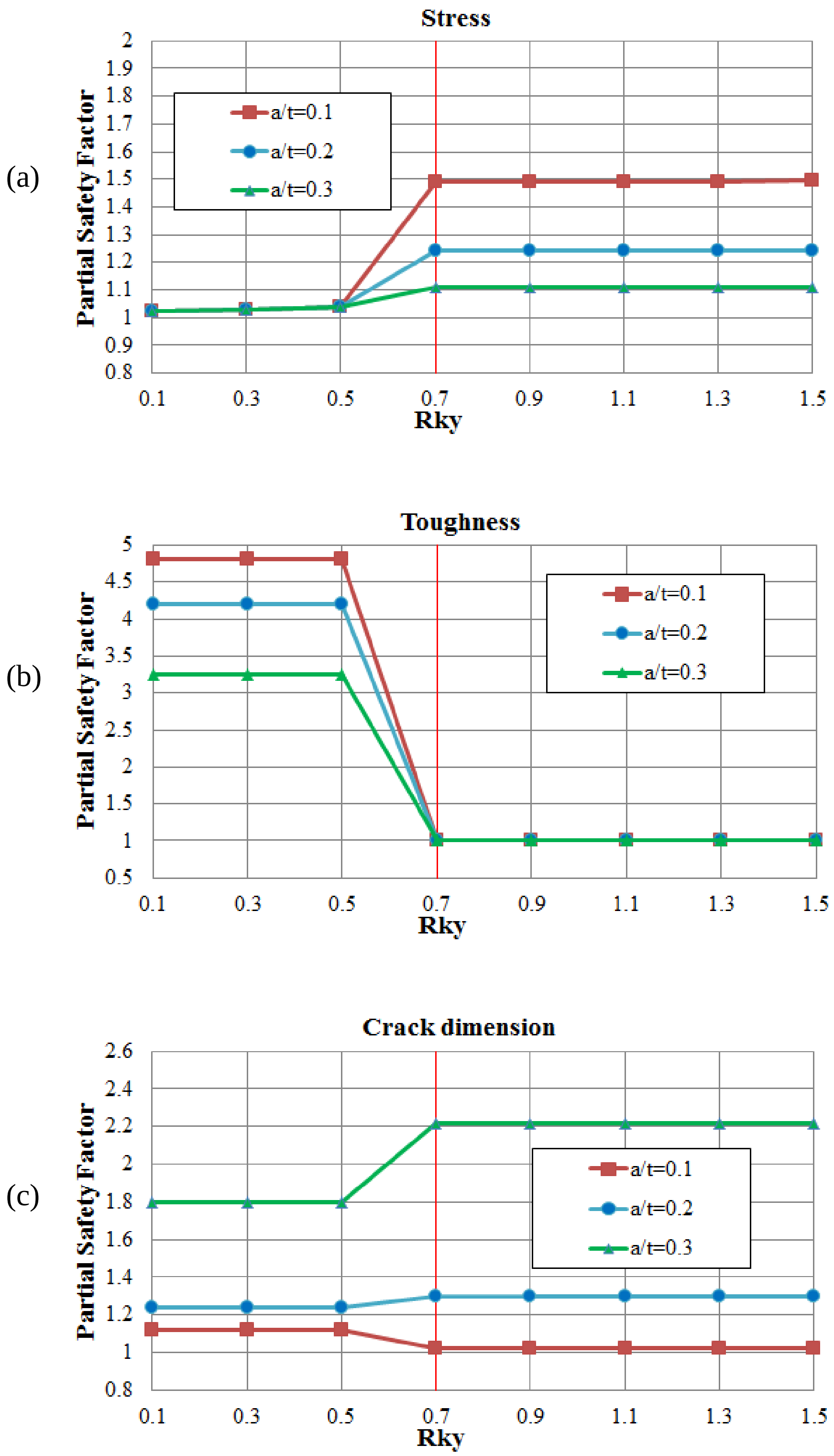

Figure 4.2 PSFs of model 2 when β_0 = 3.09, COV_S = 0.1, a/t = 0.1, 0.2, 0.3, (a) PSF of stress, (b) PSF of toughness, (c) PSF of crack dimension

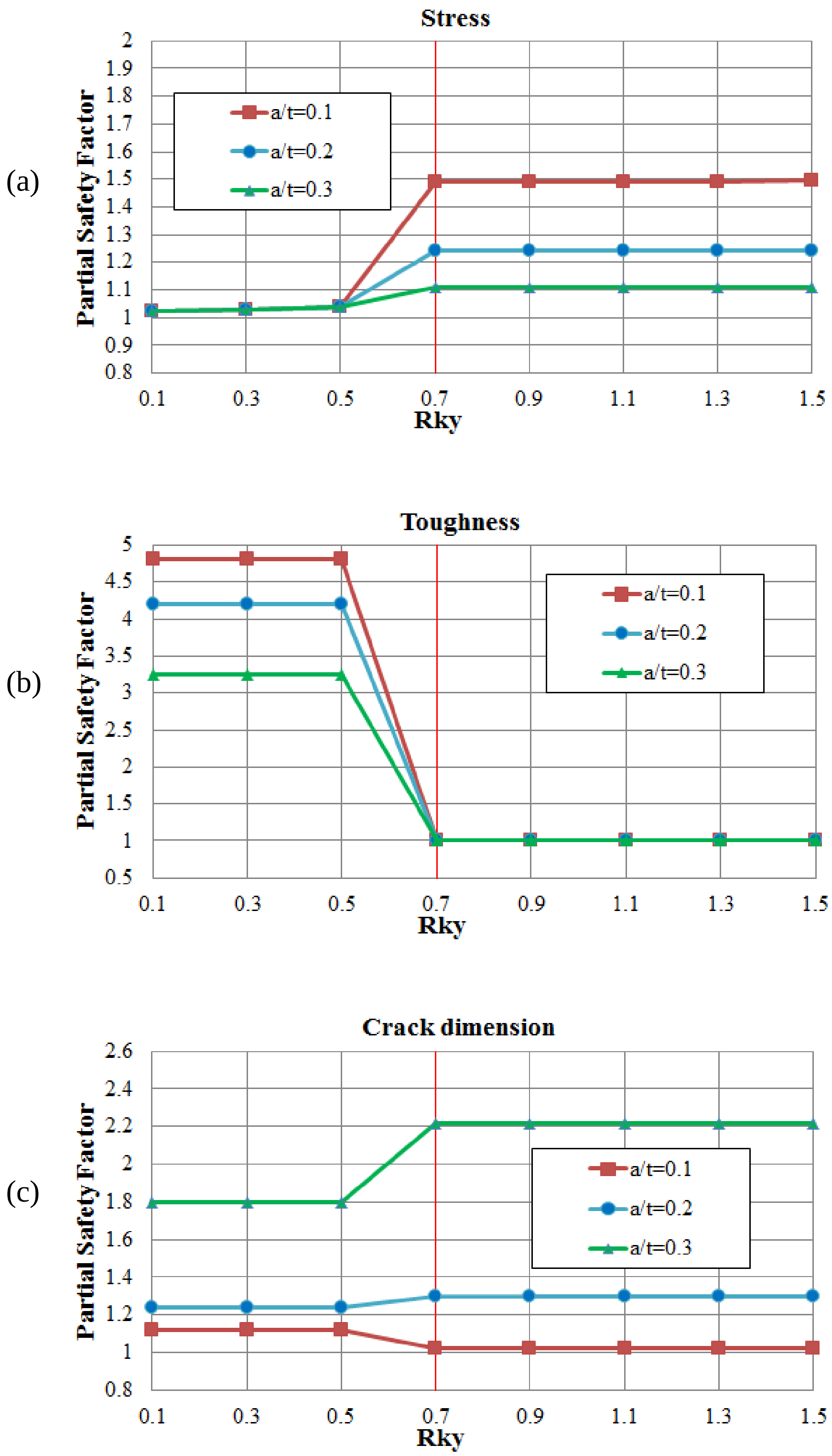

Figure 4.3 PSFs of model 3 when β_0 = 3.09, COV_S = 0.1, a/t = 0.1, 0.2, 0.3, (a) PSF of stress, (b) PSF of toughness, (c) PSF of crack dimension

We obtained that when the crack depth *a*/*t* is 0.1, the PSFs of three models are nearly the same. As a result, it is possible to apply these of PSFs of *a*/*t* = 0.1 to evaluate any model of these three.

We also calculated the PSFs of other 4 models mention in Chapter 3, and researched that when the crack depth is shallow crack (elliptical surface crack: *a*/*t* <0.3; long surface crack: *a*/*t* <0.1), for each case of determined target reliability and COV_S, the PSFs are nearly the same value. Therefore, it is possibly to generate one group of value which could be apply to evaluate all the models with an acceptably error in the result.

4.1.2 Development of new PSFs

We calculated the cases of β_0 = 2, 3.09, 4.75, COV_S = 0.1, 0.2, 0.3 and *a*/*t* = 0.01, 0.02, 0.03, ~0.3 (long crack *a*/*t* = 0.01, 0.02, 0.03, ~0.1). For each case, we recorded the PSFs in to the excel sheets and use the statistics analysis tool to take the value which has the least variation. Because in the region of plastic collapse, for the shallow cracks, the API579 PSFs has enough accuracy in the result of evaluation, we were only to check whether the PSFs calculated from real models coincide with the API579 PSFs. If they are not appreciably different, the API579 PSFs would not be substituted by new PSFs.

A statistics analysis result when β_0 = 3.09, COV_S = 0.1 is shown in Figure 4.4 and 4.5. From this analysis, we obtained the value of PSFs of this case as shown below (R_{ky}>*R*c, 1.0 is the value given the API579 PSFs).

β	**COVs**	**R_c***	**$R_{ky}<R_c$**			**$R_{ky}>R_c$**		
			PSFs	**PSFk**	**PSFa**	**PSFs**	**PSFk**	**PSFa**
3.09	**0.1**	**0.7**	**1.02**	**4.75**	**1.04**	**1.25**	**1.0**	**1.03** **(1.0)**

Using these approaches, we generated PSFs of every case, and these developed PSFs are shown in Table 4.1.

(a)

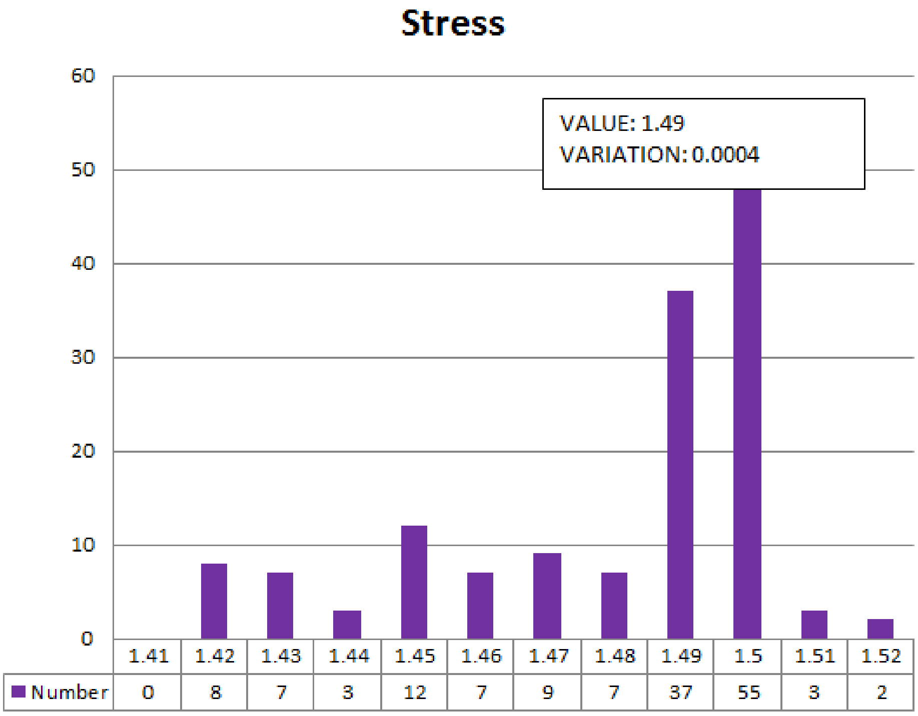
Stress
VALUE: 1.49
VARIATION: 0.0004
60
50
40
30
20
10
0
1.41 1.42 1.43 1.44 1.45 1.46 1.47 1.48 1.49 1.5 1.51 1.52
Number 0 8 7 3 12 7 9 7 37 55 3 2

(b)

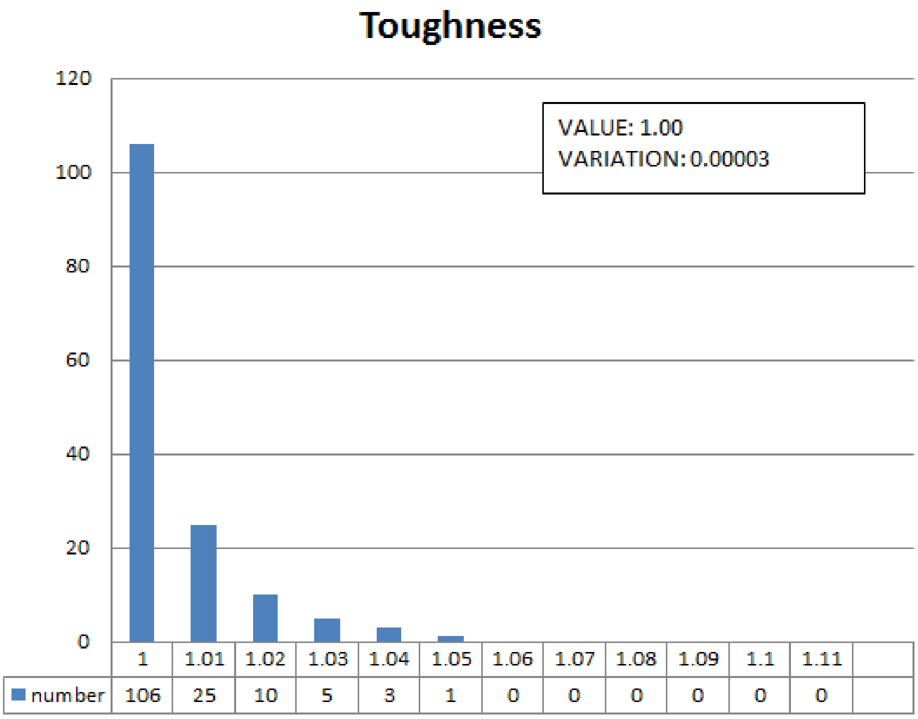
Toughness
VALUE: 1.00
VARIATION: 0.00003
120
100
80
60
40
20
0
1 1.01 1.02 1.03 1.04 1.05 1.06 1.07 1.08 1.09 1.1 1.11
number 106 25 10 5 3 1 0 0 0 0 0 0

(c)

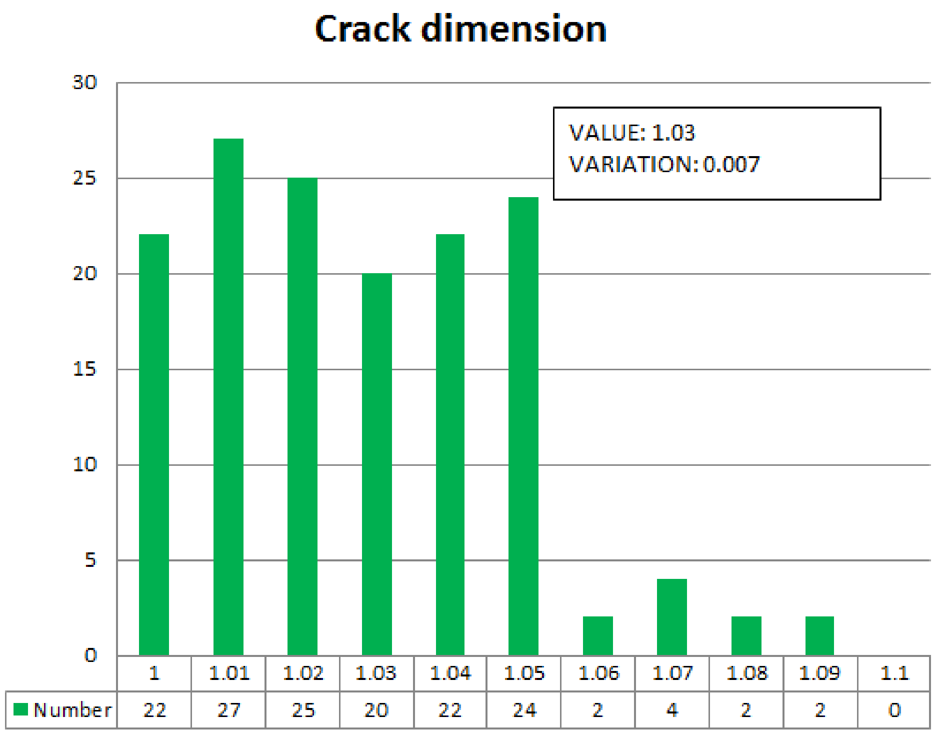

Figure 4.4 Statistic analysis of PSFs' datum (β_0 = 3.09, COV_S = 0.1, plastic collapse) of (a) stress, (b) toughness, (c) crack dimension

(a)

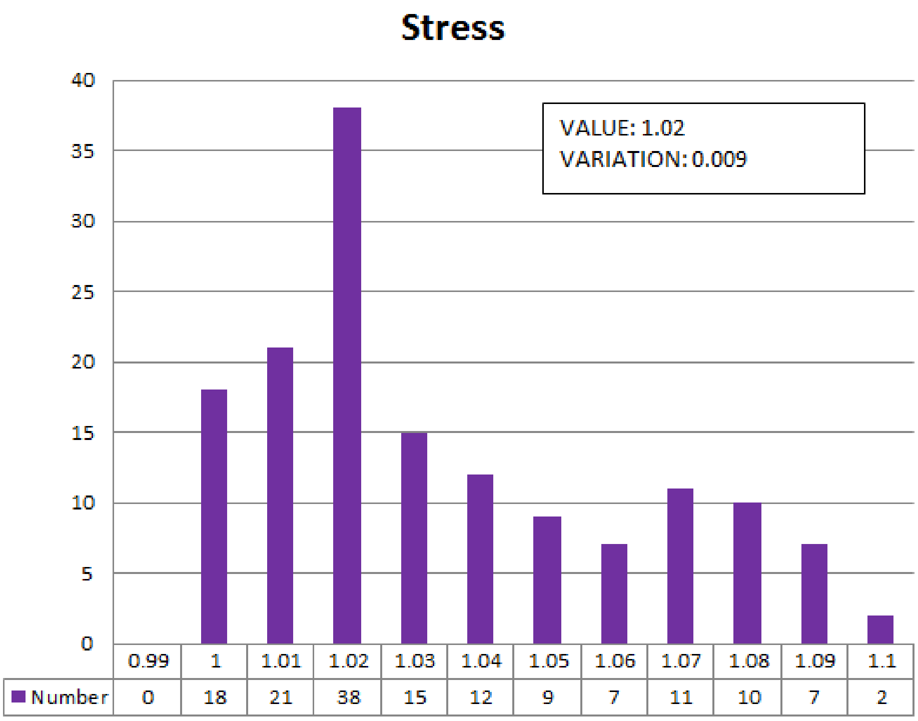

(b)

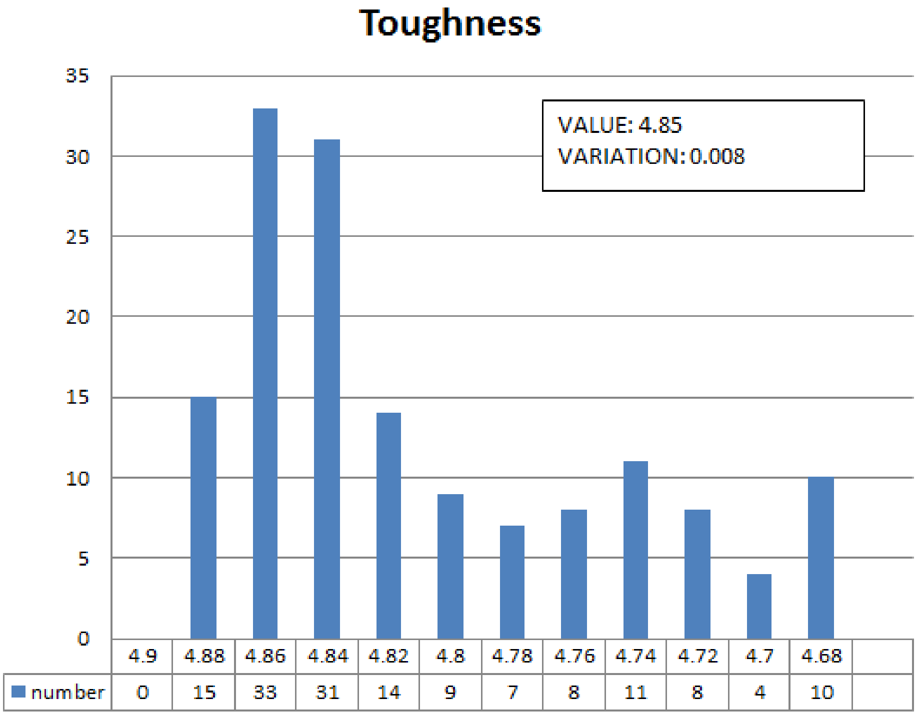

(c)

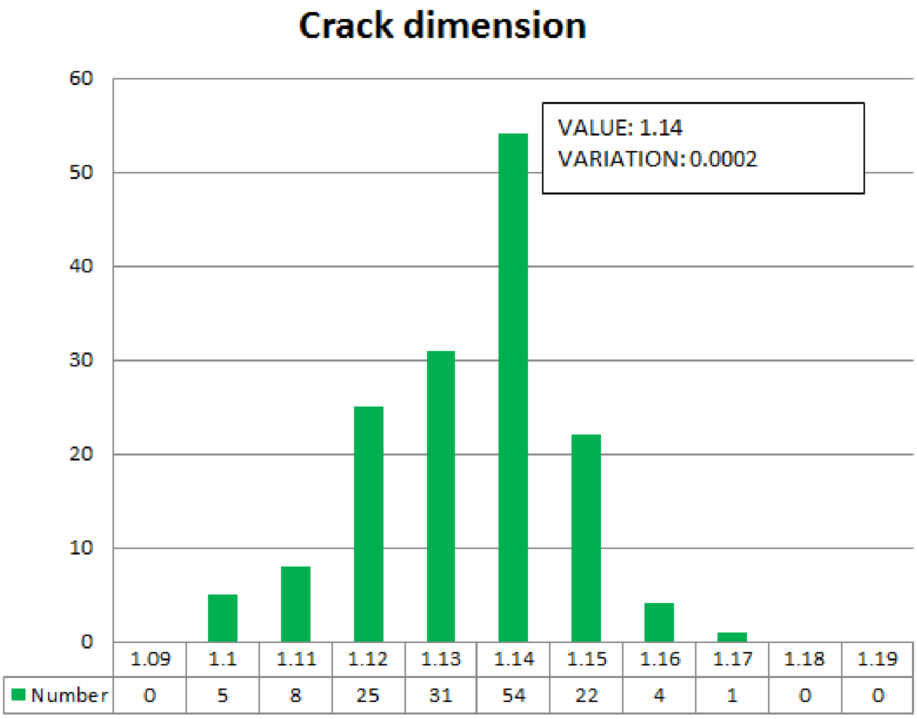

Figure 4.5 Statistic analysis of PSFs' datum (β_0 = 3.09, COV_S = 0.1, brittle fracture) of (a) stress, (b) toughness, (c) crack dimension

Table 4.1 Developed PSFs for shallow cracks

β	COVs	R_c	$R_{ky}<R_c$			$R_{ky}>R_c$		
			PSFs	PSFk	PSFa	PSFs	PSFk	PSFa
2	0.1	0.5	1.02	2.20	1.13	1.25	1	1
	0.2	0.5	1.13	2.06	1.13	1.5	1	1
	0.3	0.5	1.30	1.90	1.12	1.75	1	1
3.09	0.1	0.7	1.02	4.85	1.14	1.50	1	1
	0.2	0.7	1.13	4.51	1.12	2.0	1	1
	0.3	0.7	1.32	4.12	1.12	2.50	1	1
4.75	0.1	1.1	1.02	26.9	1.13	2.00	1	1
	0.2	1.1	1.14	25.1	1.13	3.10	1	1
	0.3	1.1	1.35	22.8	1.13	4.10	1	1

4.2 Applicability investigation of developed PSFs

An applicability investigation of PSFs given in Table 4.1 has conducted. We applied these PSFs to real model to see whether there is an improvement in the evaluation results.

The investigation results of applying these PSFs to model 1, 2, 3 are shown in Figure 4.6, 4.7 and 4.8. Here, we only show the case of COV_S=0.1 which is worst case of the categories of COV_S.

Results show that the Pf are evaluated more precisely than API579 PSFs in both of the failure regions when the component containing a shallow crack. Only at the region near the cutoff R_c, the Pf is still not evaluated correctly using these Pf. The reason is considered that near the cutoff R_c, the failure model might be unstable, the limit state function cannot reflect the limit state of this region correctly, as a result the PSFs of this region are not able to be calculated accurately. Therefore, using these PSFs may cause misestimating of Pf. It is better to perform a stress analysis to define the limit state function by the response surface method.

(a)

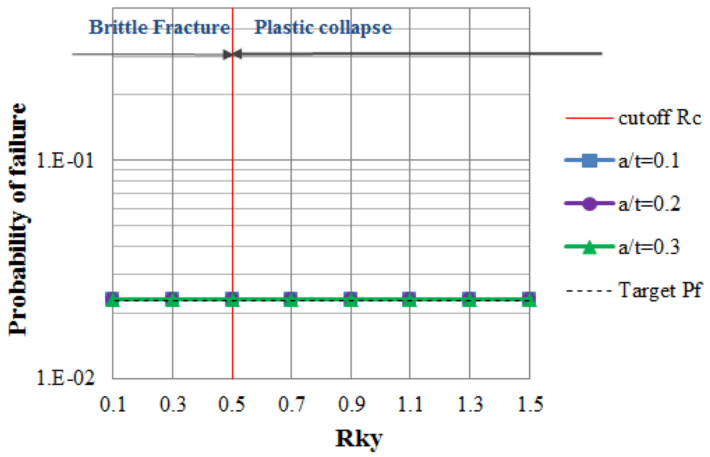

(b)

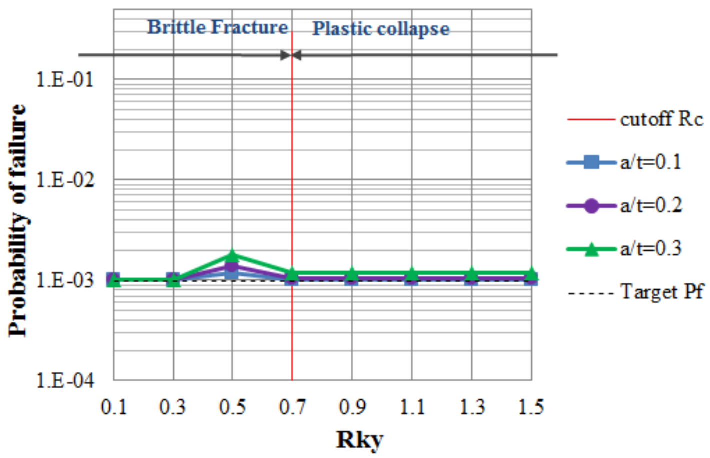

(c)

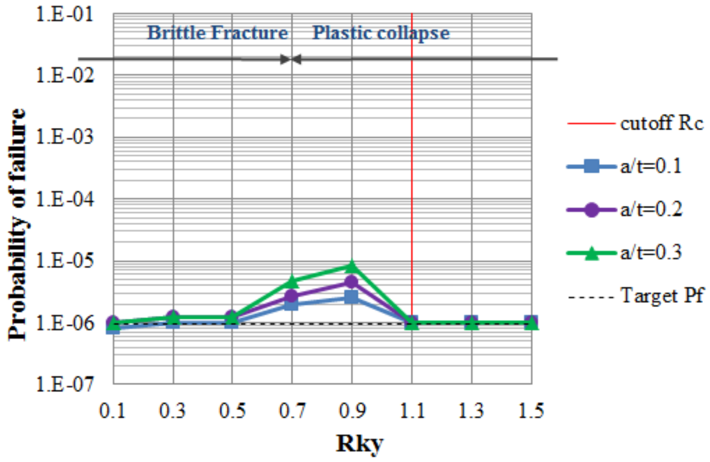

Figure 4.6 Applicability investigation of the developed PSFs on model 1 (COV=0.1)

(a) β_0 = 2.0, (b) β_0 =3.09, (c) β_0 =4.75

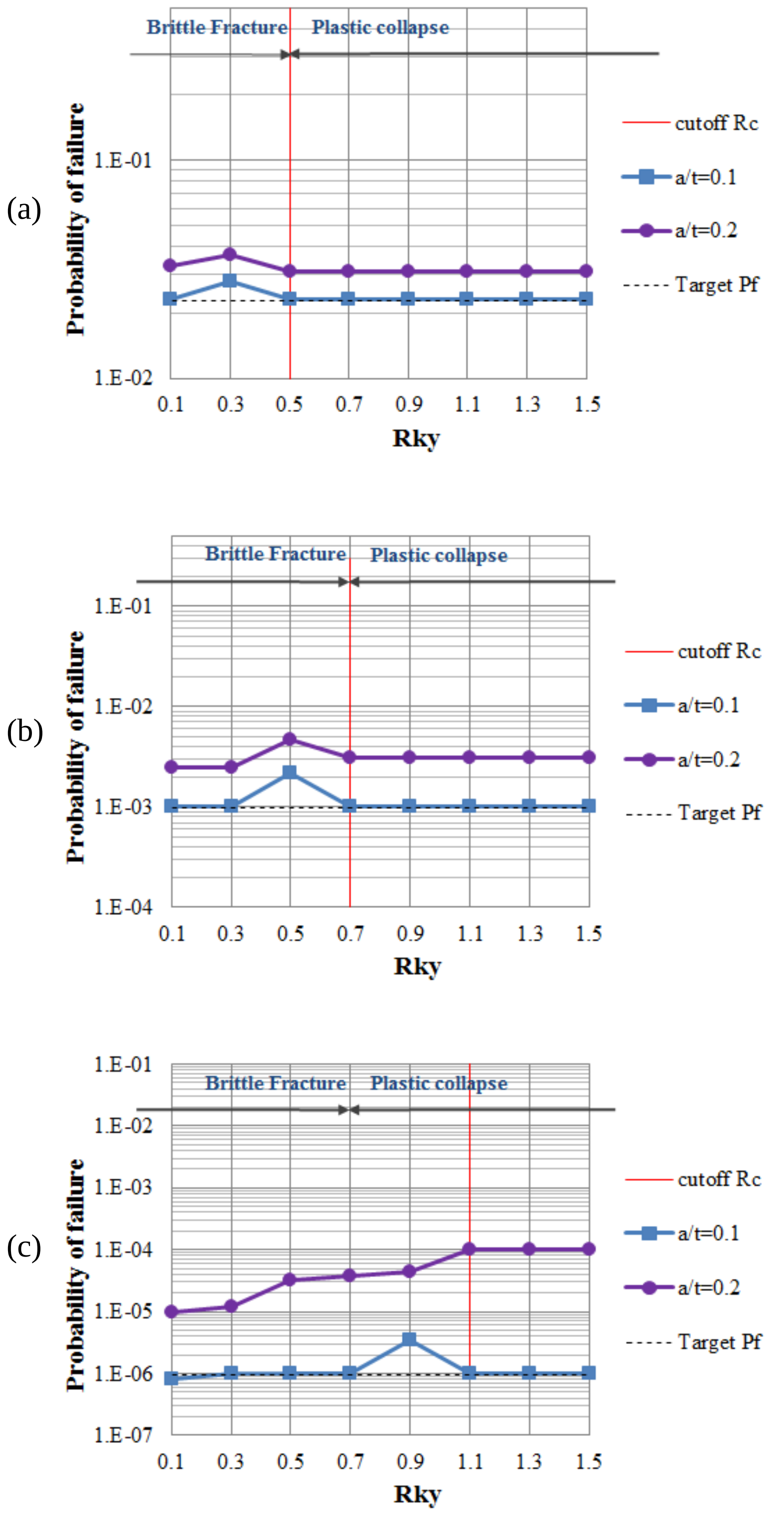

Figure 4.7 Applicability investigation of the developed PSFs on model 2 (COV=0.1)

(a) β_0 = 2.0, (b) β_0 =3.09, (c) β_0 =4.75

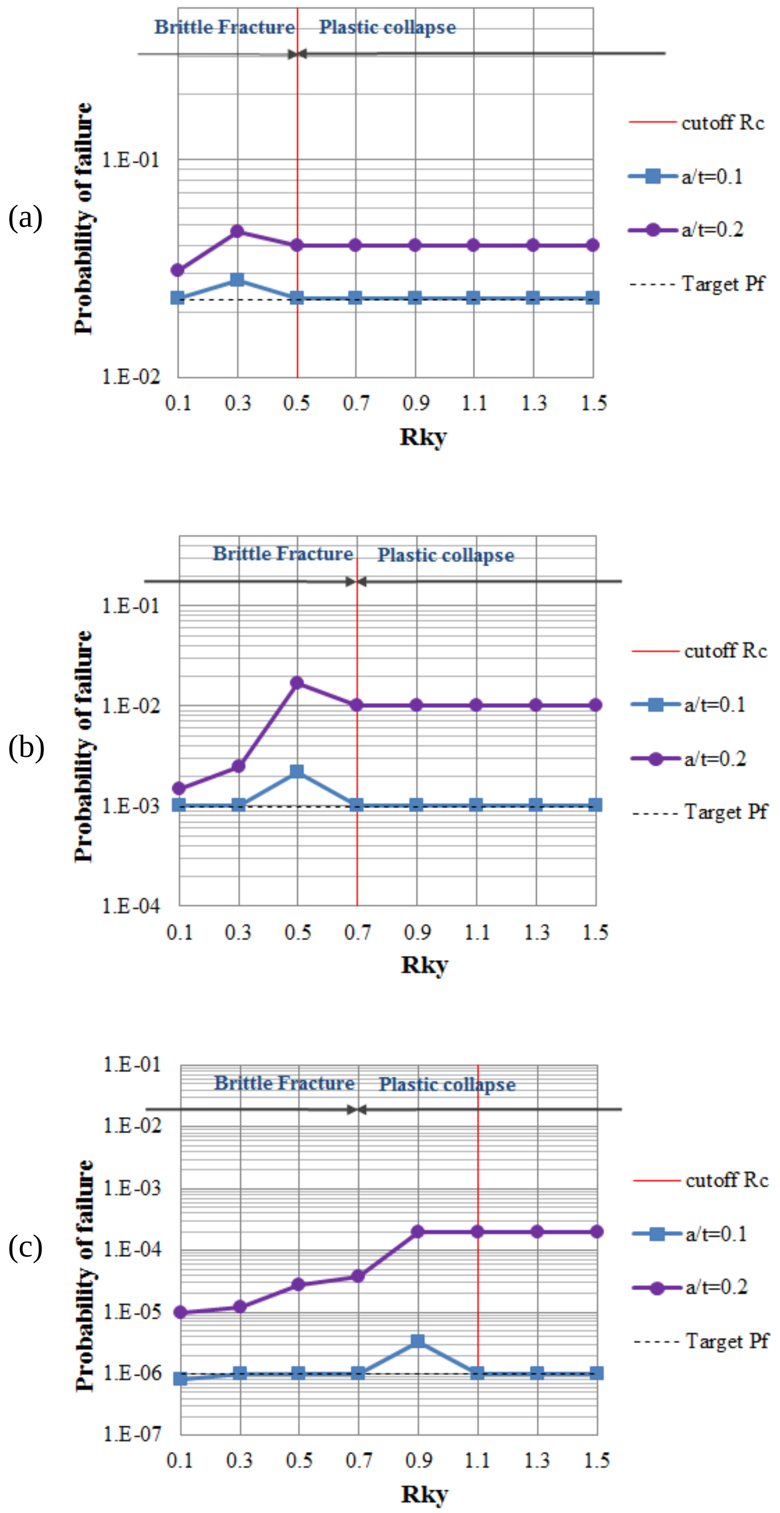

Figure 4.8 Applicability investigation of the developed PSFs on model 3 (COV=0.1)

(a) β_0 = 2.0, (b) β_0 =3.09, (c) β_0 =4.75

However, it is difficult to define the applicable region for developed PSFs by one value of crack limit depth. In order to ascertain the misestimating in the approximate evaluation using developed PSFs, it is necessary to seek out the dominant factor determining the applicability of these PSFs.

4.3 Probabilistic sensitivity

In the assessment, the various geometries of structures and cracks are expressed by the geometry indices *Y(a)* and *L(a)* which are functions of the crack dimension *a*. During seeking the design point in the FORM process, these functions of crack dimension enhanced the dependence of crack dimension on the Pf and for various geometries the affections are different. Therefore, to make clear the dependence of crack dimension on the Pf for different models is helpful to determine the applicable region of developed PSFs.

Probabilistic sensitivity α is used to measure the dependence of variation of independent variables on the Pf.

$$\alpha_i = \frac{\delta Pf}{\delta x_i}\frac{\sigma_{x_i}}{\sigma_{Pf}} = \frac{\partial Pf}{\partial x_i}\frac{\sigma_{x_i}}{\sigma_{Pf}} \tag{4.1}$$

Equation 4.1 [5] can be conducted to

$$\alpha_i = \frac{\partial Pf}{\partial \beta}\frac{\partial \beta}{\partial x_i}\frac{\sigma_{x_i}}{\sigma_{Pf}} = -\phi(\beta)\frac{x_i}{\sigma_{x_i}\sqrt{\sum x_i^2}}\frac{\alpha_i^*}{\phi(\beta)} = -\alpha_i^* \tag{4.2}$$

where the α_i^* is the direction cosine which is a production of the reliability method.

By plotting the values of probabilistic sensitivity of various models and various COV_S, we obtained the relation between the sensitivity and Pf. It is shown that when the sensitivity of crack dimension is low, the probability of failure maintains a small value nearly agreeing with the target Pf. However when the sensitivity increases to a high value, the Pf increases obviously that the underestimating of Pf might reaches ten or thousands times than target. Also, this is also an explanation for that why the applicability is influenced by the COV_S. When the COV_S is chosen a high level, the variation of stress had more influence on the Pf, relatively the influence of crack dimension is weakened and sensitivity decreased, final the Pf got closer to target Pf lines [6].

Using the sensitivity to define the applicable region of developed PSFs hasn't been a practicable method yet, because the sensitivity requires performing a reliability method (probabilistic analysis), which might be difficult in same cases. However, this conclusion

(a)

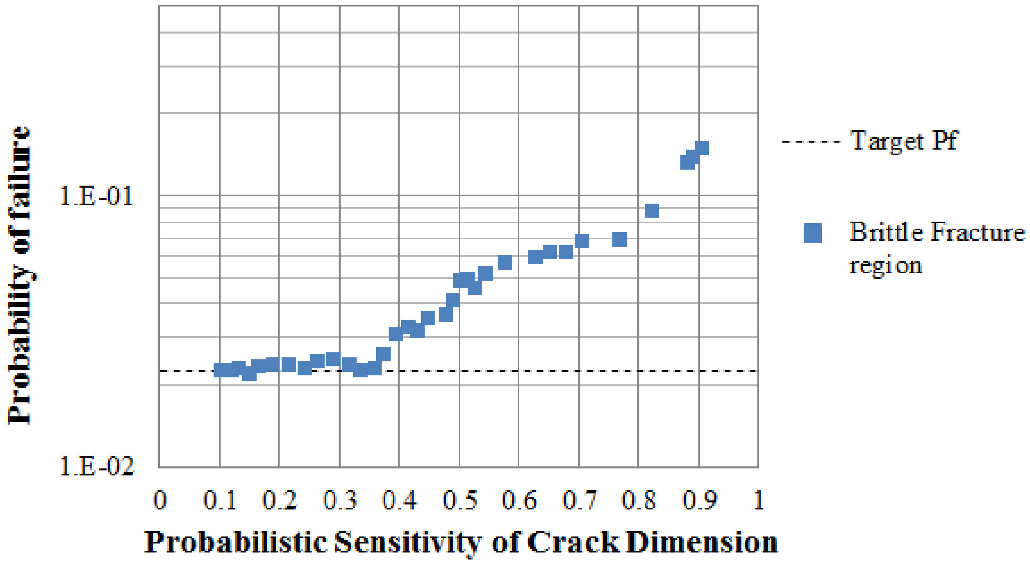

(b)

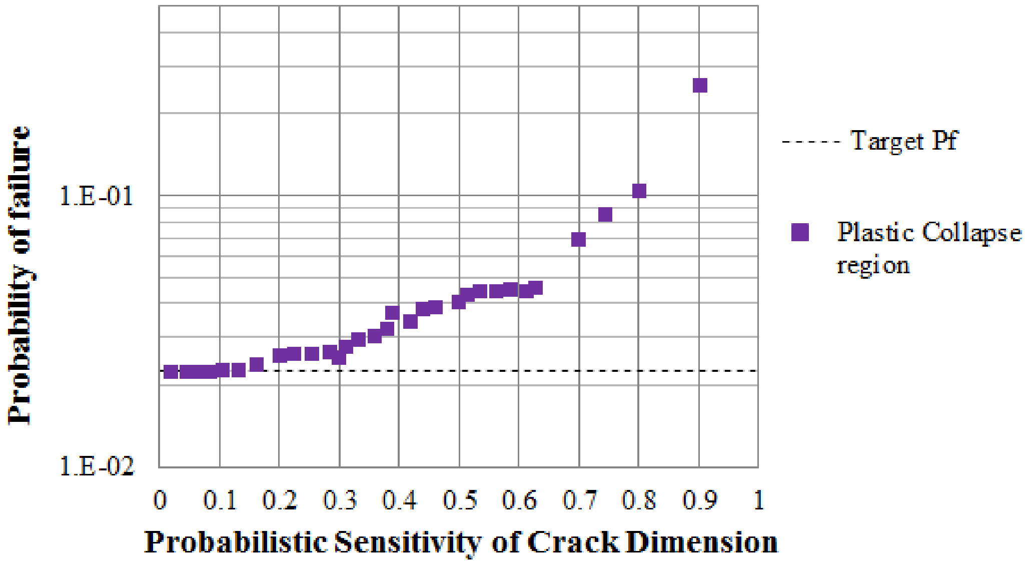

Figure 4.9 Dependence of crack dimension on the probability of failure (β_0=2.0)

(a) brittle fracture region, (b) plastic collapse region

(a)

(b)

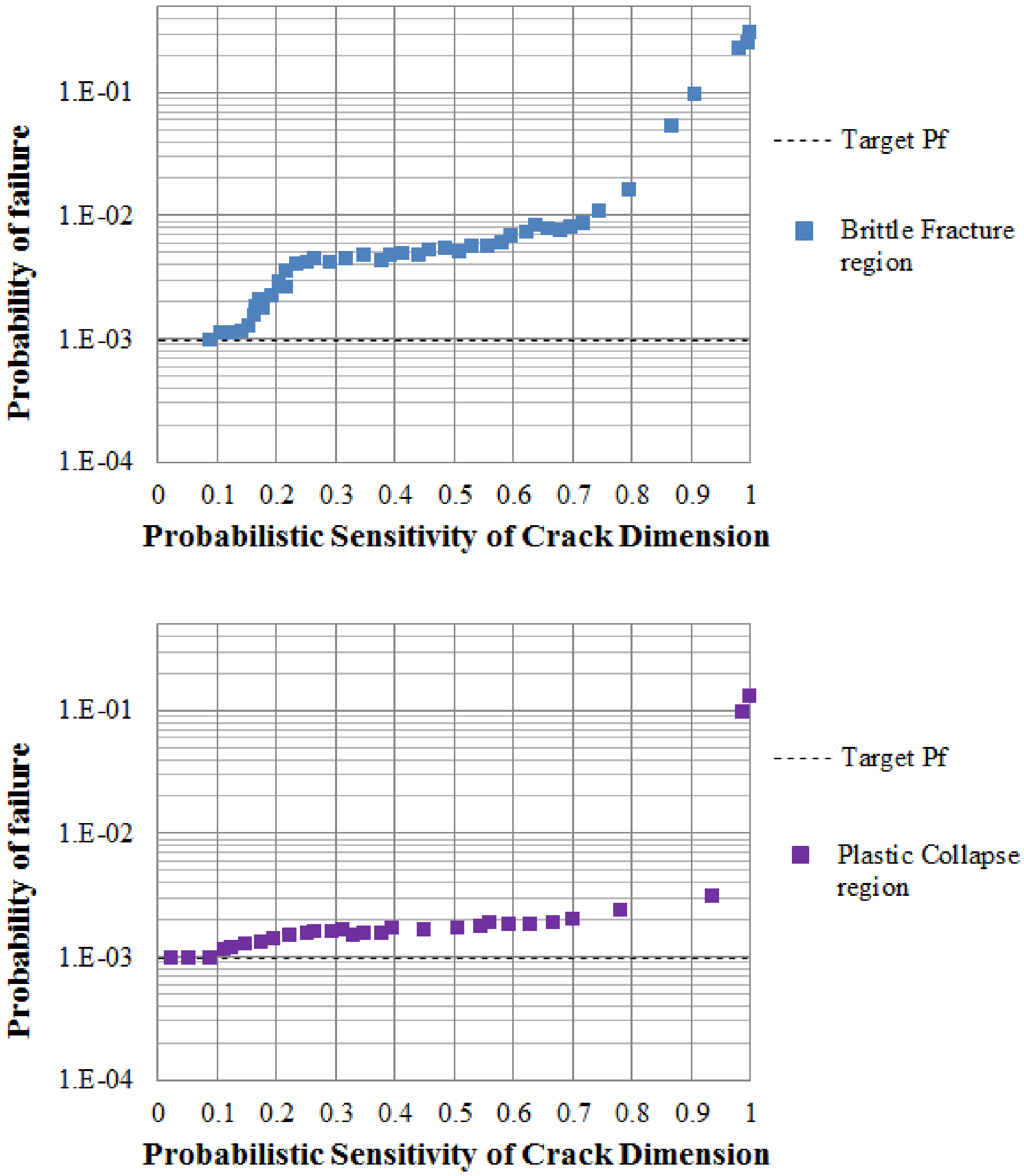

Figure 4.10 Dependence of crack dimension on the probability of failure (β_0=3.09)

(a) brittle fracture region, (b) plastic collapse region

(a)

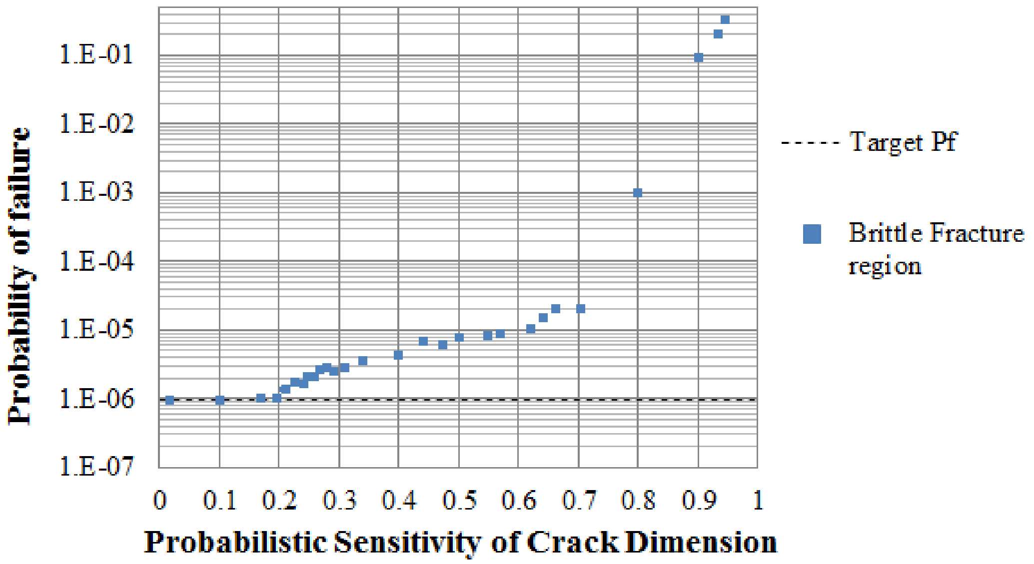

(b)

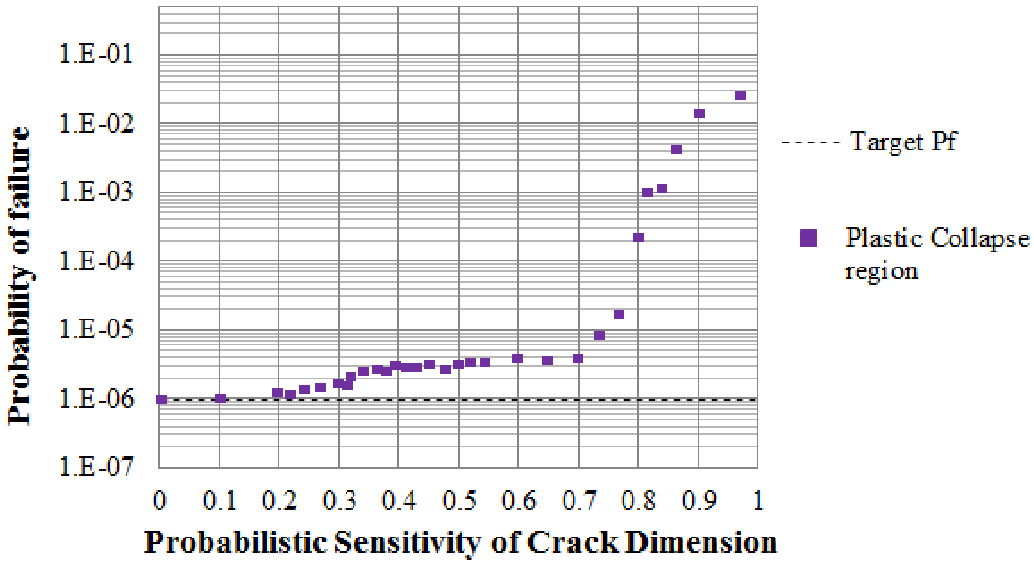

Figure 4.11 Dependence of crack dimension on the probability of failure (β_0=3.09)

(a) brittle fracture region, (b) plastic collapse region

Chapter 5. Conclusions

Applicability of partial safety factors given in API 579

In this paper, we investigated the applicability of API579 PSFs for real models. The results showed that, when the failure mode is plastic collapse (R_{ky}>R_c,), the API579 PSFs are able to evaluate the component containing shallow cracks for the real models with various geometries of structure and crack. However, with the increase depth of crack, these result of the approximate evaluation becomes less precise, the API579 PSFs should not be used in the evaluation. On the other hand, when the failure mode is brittle fracture (R_{ky}<R_c,), there is extreme mistake in the assessment result that these PSFs are not applicable to real models for either shallow or deep cracks.

Development of new partial safety factors

As the API579 PSFs are not applicable in some cases, we developed a new group of PSFs. These PSFs are generated statistically from the PSFs evaluated from real models by first order reliability method. It has been shown that, these PSFs could provide a more accurate evaluation than API579 PSFs when the brittle fracture is the failure model. However, it is hard to generate a group of PSFs which can be used in the evaluation for components containing a deep crack. We suggest that for a deeper crack, it is better to conduct a probabilistic analysis rather than approximate evaluation.

We also found the dominant factor of sensitivity of crack dimension which determines the applicability of new PSFs. Although this result cannot be used as a quantitative measurement of the applicability, it still provides help to reduce the misestimating in the approximate evaluation by improving the degree of accuracy of the variables' datum.

Acknowledgements

First and foremost, I would like to express my heartfelt gratitude to my advisor Professor Shinsuke SAKAI and Professor Satoshi IZUMI for giving me the chance to conduct research at this laboratory, and the valuable guidance in every stage of the writing of this thesis. Without their enlightening instruction, impressive kindness and patience, I could not have completed my thesis.

I would also like to extend my thanks to Mr. Junki MAEDA, Mr. Takuyo KAIDA for their kindness helps. I would also like to thank the stuffs in my laboratory, especially Miss. Asuka HATANO, and Mr. Hiro TANAKA who have helped me to develop the fundamental and essential academic competence.

Last but not least, I would like to thank all the members in Sakai-izumi laboratory, thank them for being kind, friendly and welcoming to me, and also thanks their encouragement and support.

Reference

1. Osage D.A., Wirsching P. H. and Mansour A.E., Application of Partial Safety Factors For Pressure Containing Equipment, *ASME Pressure Vessel and Piping Conference*,(2000).
2. API, Fitness-for-Service ,API 579-1/ASME FFS -1(2007)
3. Yuichi MOGAMI, Shinsuke SAKAI and Tetsuya SASAKI, Evaluation of Structural Integrity with Partial Safety Factor Method, 2009
4. Amin Muhammed, Background to the derivation of partial safety factors for BS 7910 and API 579, *Engineering Failure Analysis 14*, (2007), pp.481-488.
5. 戒田　拓洋, 最上　雄一, 泉　聡志, 酒井　信介, API 579-1/ASME FFS -1の局部減肉評価基準への信頼性手法の適用, *日本機械学会論文集A編, Vol.77, No.777*, p.P736-740*(2011)*
6. Qiang QU, Satosi IZUMI, Shinsuke SAKAI, Applicability of FFS Assessment Using Partial Safety Factors Evaluated by Infinite Plate, *ASME Pressure Vessel and Piping Conference*,(2013).

Development of Fitness-For-Service Assessment Method Based on Reliability

信頼性に基づく構造健全性評価手法の開発

116907

Qiang QU